Molecular Imaging of gene expression and protein function in vivo with PET and SPECT

ARTICLE *in* JOURNAL OF MAGNETIC RESONANCE IMAGING · OCTOBER 2002

Impact Factor: 3.21 · DOI: 10.1002/jmri.10182 · Source: PubMed

3 AUTHORS, INCLUDING:

Vijay Sharma
Malaviya National Institute of Technology J…
62 PUBLICATIONS **1,972** CITATIONS
SEE PROFILE

Gary D Luker
University of Michigan
134 PUBLICATIONS **5,291** CITATIONS
SEE PROFILE

JOURNAL OF MAGNETIC RESONANCE IMAGING 16:336–351 (2002)

Invited Review

Molecular Imaging of Gene Expression and Protein Function In Vivo With PET and SPECT

Vijay Sharma, PhD, Gary D. Luker, MD, and David Piwnica-Worms, MD, PhD*

Molecular imaging is broadly defined as the characterization and measurement of biological processes in living animals, model systems, and humans at the cellular and molecular level using remote imaging detectors. One underlying premise of molecular imaging is that this emerging field is not defined by the imaging technologies that underpin acquisition of the final image per se, but rather is driven by the underlying biological questions. In practice, the choice of imaging modality and probe is usually reduced to choosing between high spatial resolution and high sensitivity to address a given biological system. Positron emission tomography (PET) and single-photon emission computed tomography (SPECT) inherently use image-enhancing agents (radiopharmaceuticals) that are synthesized at sufficiently high specific activity to enable use of tracer concentrations of the compound (picomolar to nanomolar) for detecting molecular signals while providing the desired levels of image contrast. The tracer technologies strategically provide high sensitivity for imaging small-capacity molecular systems in vivo (receptors, enzymes, transporters) at a cost of lower spatial resolution than other technologies. We review several significant PET and SPECT advances in imaging receptors (somatostatin receptor subtypes, neurotensin receptor subtypes, $\alpha_v\beta_3$ integrin), enzymes (hexokinase, thymidine kinase), transporters (*MDR1* P-glycoprotein, sodium-iodide symporter), and permeation peptides (human immunodeficiency virus type 1 (HIV-1) Tat conjugates), as well as innovative reporter gene constructs (herpes simplex virus 1 thymidine kinase, somatostatin receptor subtype 2, cytosine deaminase) for imaging gene promoter activation and repression, signal transduction pathways, and protein-protein interactions in vivo.

Key Words: positron emission tomography; single-photon emission computed tomography; reporter gene; thymidine kinase; P-glycoprotein; fluorodeoxyglucose; protein-protein interactions
J. Magn. Reson. Imaging 2002;16:336–351.

Molecular Imaging Center, Mallinckrodt Institute of Radiology and Department of Molecular Biology and Pharmacology, Washington University Medical School, St. Louis, Missouri.

Contract grant sponsor: U.S. National Institutes of Health; Contract grant number: P50 CA94056; Contract grant sponsor: Department of Energy; Contract grant number: DE FG02 94ER61885.

*Address reprint requests to: D.P.-W., Molecular Imaging Center, Mallinckrodt Institute of Radiology, Washington University Medical School, 510 S. Kingshighway Blvd., Box 8225, St. Louis, MO 63110. E-mail: piwnica-wormsd@mir.wustl.edu

Received March 27, 2002; Accepted June 26, 2002.
DOI 10.1002/jmri.10182
Published online in Wiley InterScience (www.interscience.wiley.com).

WITH A FIRST DRAFT OF THE HUMAN genome completed (1) and a refined map under way, sequencing of the human genome is expected to lead to new medical therapies, diagnostics, and ultimately cures previously not imagined. In this emerging postgenomic era, wherein functionality will be added to this vast array of genetic information, opportunity exists for imaging to play a significant role in basic, translational, and clinical research as related to functional genomics. Herein, the overall objective is focused on adding function through molecular imaging. The goal is to advance our understanding of biology and medicine through noninvasive in vivo investigation of the cellular and molecular events mediating normal physiology and pathologic processes.

Molecular imaging is focused on monitoring gene expression in vivo. The target genes can be either endogenous or exogenous. To meet the goal of monitoring endogenous genes in vivo, a strategic choice must be made regarding whether it is best to image DNA per se, messenger ribonucleic acid (mRNA) transcripts, the protein product of gene expression, or functional activity of the expressed protein. The best strategy may depend on the biochemical context of the target gene under investigation and the desired end point of the study. Similarly, for monitoring exogenous gene (transgene) expression in vivo, the choice of measuring DNA, mRNA, protein, or function is fundamental to designing optimal imaging strategies and probes. Ultimately, these choices will be influenced by the characteristics of the biological pathways and their potential as imaging targets in vivo.

One consideration relates to the number of target molecules and their impact on generating sufficient signal-to-noise ratios. For example, direct imaging of DNA would require imaging just two molecules per cell, a considerable challenge for remote imaging devices: positron emission tomography (PET), single-photon emission computed tomography (SPECT), magnetic resonance imaging (MRI), and optical imaging. Furthermore, any two DNA molecules may not be identical (heterologous polymorphisms), and there exists considerable sequence variability between individuals and across species. Nonspecific and nontarget binding of imaging probes are likely to overwhelm specific signals arising from target DNA. In addition, direct imaging of DNA provides no information as to whether that gene is actually expressed and contributing to the physiologi-

cal state of the imaged cell or tissue. Similarly, mRNA is typically present at only 50 to thousands of molecules per cell, and again, direct imaging approaches requiring one-to-one correlation with the target molecules (e.g., antisense) face considerable challenges (2). However, in contrast to DNA, imaging mRNA will reveal information relevant to the patterns of genes expressed during the imaging study. Proteins can be present at significantly higher levels, perhaps thousands to millions of copies per cell, and thus direct imaging of proteins is achieved readily. Indeed, direct molecular imaging of receptor subtypes with radiopharmaceuticals is already a laboratory and clinical reality (e.g., somatostatin-2 receptor (SSTR2) imaging with ^{111}In-Octreoscan or GPIIb/IIIa receptor imaging with ^{99m}Tc-Acutech (3,4)). Finally, imaging protein function has the potential for massive signal amplification when the target protein is, for example, an enzyme that can magnify the signal through metabolic conversion of a precursor substrate or trap a substrate or prodrug within an intracellular compartment. The action of the sodium-iodine transporter to trap radiolabeled iodine within the thyroid gland may be one of the earliest examples of "molecular imaging" through exploitation of the selective trapping of a specific compound (^{131}I) by the concentrative compartmentalization of a labeled target agent relevant to the metabolic pathway under investigation (5). Building on this concept, molecular imaging as now envisioned actually exploits creative synergies between these hierarchies of signal sources, resulting in fusions between these biological scales. For example, it is now feasible to exploit enzymatic amplification of protein function to amplify characteristic signals arising from promoters driving expression of specific DNA sequences. Thus, creative design, application, and validation of fusion constructs and incorporation of molecular biology techniques into the research process are important aspects of molecular imaging.

One underlying premise of molecular imaging is that this emerging field is not defined by the imaging technologies that underpin acquisition of the final image per se, but rather is driven by the underlying biological questions (6). Thus, selection of an imaging technology will be driven primarily by the biological question and the advantages of a specific imaging modality, rather than attempting to use one technique for all investigations. In addition, most (but not necessarily all) molecular imaging approaches make use of image-enhancing or contrast agents that provide molecular specificity to the imaging signal. These have inherent physicochemical differences, producing their respective image contrasts that in turn provide advantages or limitations for certain types of molecular imaging queries. In practice, choice of imaging modality and probe usually reduce to choosing between high spatial resolution and high sensitivity. For example, MRI and contrast agents that affect relaxivity inherently provide higher spatial resolution than PET or SPECT imaging. However, because of the indirect nature of enhancement produced by MR contrast agents, higher concentrations of material, on the order of 10–100 micromolar concentrations and higher, generally are necessary to produce sufficient image contrast. These pharmacological levels of compound result in a stringent standard for MR contrast agents in regard to real-world risks of potential toxicity, cross-reactivity, and pharmacodynamic effects of the agents in vivo. Pharmacologic concentrations of contrast agents also may perturb the molecular signal that is being monitored by MRI. Conversely, PET and SPECT agents inherently are synthesized at sufficiently high specific activity to enable use of tracer concentrations of compound (picomolar to nanomolar) for detecting molecular signals while providing the desired levels of image contrast. However, the physics of gamma ray detection result in lower spatial resolution. Thus, when high spatial resolution is desired, MRI may provide certain advantages for selected molecular imaging hypotheses, while tracer technologies provide high sensitivity for imaging low-capacity systems. Similar concepts and trade-offs could be extended to ultrasound contrast agents, bioluminescence and optical imaging techniques, and even x-ray contrast agents. Because the goal of molecular imaging is to interrogate specific molecular signals, the underlying biological question, rather than the technology itself, should drive the choice of imaging technology.

To begin to investigate molecular signals in vivo, researchers already have developed and characterized methods for imaging endogenous proteins, such as receptors, transporters, or enzymes and their respective functions. More recently, methods also have been validated to analyze the specific expression of a transgene of interest, typically by quantifying the activity of genes delivered by a viral vector as would be used in gene therapy or an exogenous reporter gene. In the following sections, we will review several principles of selected applications of radiotracer technologies for molecular imaging with PET and SPECT. Much of the current focus in molecular imaging is directed toward oncological applications, and thus the reader may perceive a cancer bias in this review. However, molecular imaging by PET and SPECT can and does extend to any and all areas of biomedical research. Indeed, the reader is encouraged to explore recent reviews that summarize research activity in PET and SPECT radiochemistry and the pharmacokinetics of radiolabeled agents, especially with regard to neurobiology, having as a goal by any definition molecular imaging (7–13).

MOLECULAR IMAGING OF ENDOGENOUS PROTEIN FUNCTION IN VIVO

Glucose Transporters and Hexokinase

PET with 2-[^{18}F]fluoro-2-deoxy-D-glucose (FDG) (Fig. 1) may be characterized as one of the first "molecular imaging" techniques validated in the basic sciences as well as in a clinical setting. Indeed, the tracer FDG is used more commonly in most PET centers to image the high glycolytic rates of many cancers than the metabolic activity of the brain (14). Warburg recognized the increased rates of glycolysis present in tumors over 70 years ago (15). Hexokinase catalyzes the initial, rate-limiting step in glycolysis, which is phosphorylation of glucose to glucose-6-phosphate. FDG, an analog of glucose, enters cells through the same pathways of facilitated diffusion as glucose, i.e., via glucose transporters Glut1 and Glut4, and is subsequently phosphorylated

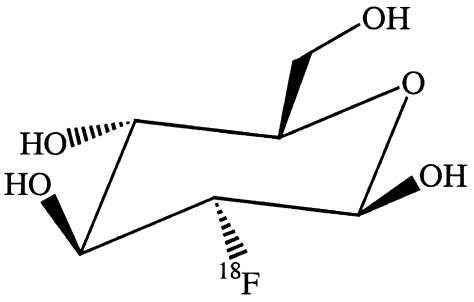

FDG

Figure 1. Structure of [^{18}F]FDG.

by hexokinase. However, FDG-6-phosphate is not further metabolized significantly and, because it is negatively charged, remains trapped within cells. Imaging of hexokinase activity can be achieved by incorporating [^{18}F] into FDG, enabling detection of the trapped, phosphorylated metabolite by PET. Pharmacological doses of FDG actually inhibit glycolysis in vivo, but imaging with this compound can be performed safely because only tracer amounts are needed for PET.

As discussed by Wahl et al (14), the transport kinetics of FDG across tumor cell membranes potentially can also affect the final imaging signal. The importance of transport of FDG has been well shown in the myocardium and skeletal muscle (14). It also has been shown by several groups that Glut1 protein levels are increased on the cell surface of many cancer cells (16,17). Glut1 levels also are increased by placing cells in a hypoxic environment (18). In hypoxia, accumulation of FDG and accumulation of FDG-6-phosphate increase as glucose transporter levels increase. While hexokinase activity may also change, an adaptive response of hypoxic tumor cells is increased expression of glucose transporters on the surface. This phenomenon likely preserves glucose metabolism at levels needed for survival. Several groups have shown that the tumor cells with highest levels of Glut1 expression are located in what are apparently hypoxic areas of tumors, near necrotic regions (19,20). Thus, glucose transporter levels can affect tissue uptake of FDG.

Studies performed in vitro and in animals with breast cancer have shown that FDG uptake in tumors is positively correlated with Glut1 levels and with the number of viable cancer cells (19). To date, correlation of FDG uptake with Glut1 expression levels has been better than with hexokinase levels, but neither is precisely correlated (21). Another complexity known from animal studies is that FDG uptake is not unique to cancer cells. Since FDG broadly traces glucose metabolism rather than tumor-specific glucose metabolism, FDG uptake can occur into other glucose-utilizing cells, such as macrophages and leukocytes (22). This uptake can be confusing in clinical interpretation of images, but nonetheless illustrates that the underlying biochemical mechanism is being properly mapped.

Imaging of "tumor metabolism" with FDG is a widely used method for detecting a specific molecular target in vivo, and this radiotracer has an established clinical utility for detection of normal and pathologic function in brain and heart. Additionally, imaging with PET and FDG is becoming increasingly important in the diagnosis and management of patients with cancer, particularly for detection of metastatic disease (reviewed in Hoekstra et al (23)). Several groups have shown the feasibility of FDG for targeting animal tumors and human tumor xenografts of a variety of types, and now there is an extensive clinical literature showing efficacy of PET with FDG in the detection of a variety of human tumors (23–26). In the context of molecular imaging in oncology, imaging with FDG fulfills all criteria for selective imaging of a specific enzymatic activity, but is limited per se in that the target enzyme, hexokinase, is not specific for cancer. Thus, the success of the approach does not reside in a high degree of selectivity in terms of the expression pattern of the molecular target, but rather, the clinical utility is manifest in the enhanced functional activity of hexokinase (and transport) displayed in malignancy. Nonetheless, imaging with FDG could be considered the first routine clinical molecular imaging procedure performed using dedicated quantitative PET devices.

Cell Proliferation and Endogenous Thymidine Kinase

As indicated above, because FDG PET is not selective for tumor cells, investigators have sought more direct measures of tumor progression with a focus on cell proliferation, one hallmark of cancer (27). One approach has been use of radiolabeled thymidine, a method that has been used for years in cell culture and animal studies to assess cell proliferation. Rapidly incorporated into newly synthesized DNA, thymidine analogs radiolabeled with PET isotopes can provide images of tumor cell proliferation. Some of the first experiments were performed with ^{11}C-thymidine labeled in the methyl position (28) and later in the ring-2 position (29). However, the short half-life (20 minutes) of ^{11}C impaired application of this and related ^{11}C-labeled thymidine analogs (30). In addition, these radiopharmaceuticals were found to be rapidly and differentially degraded in vivo, generating complexities in analysis because of substantial contributions from radiolabeled metabolites (31). Thus, many investigations focused on the goal of identifying a pyrimidine analog that was resistant to degradation and could be labeled with longer-living isotopes, such as ^{18}F (half-life, 110 minutes), ^{124}I (half-life, 4.2 days), or ^{76}Br (half-life, 16 hours). Among these were [^{124}I]IUdR and [^{76}Br]BrUdR, but because they were not thymidine, there was concern that net uptake in tissues may not directly reflect the rate of thymidine precursor incorporation in DNA (31). Several ^{18}F-labeled analogs also have been synthesized. Many were found to be poor proliferation tracers because of trapping in RNA pools or insufficient concentration in proliferating tissues, but two compounds have shown promise: ^{18}F-labeled 3′-deoxy-3′-fluorothymidine (FLT) (32) and 1-(2′-fluoro-2′-deoxy-β-D-ribofuranosyl)thymidine ([^{18}F]FMAU) (30,33). FLT and FMAU (Fig. 2) are transported into cells by the nucleoside transporter family and phosphorylated by endogenous thymidine kinase (TK), leading to intracel-

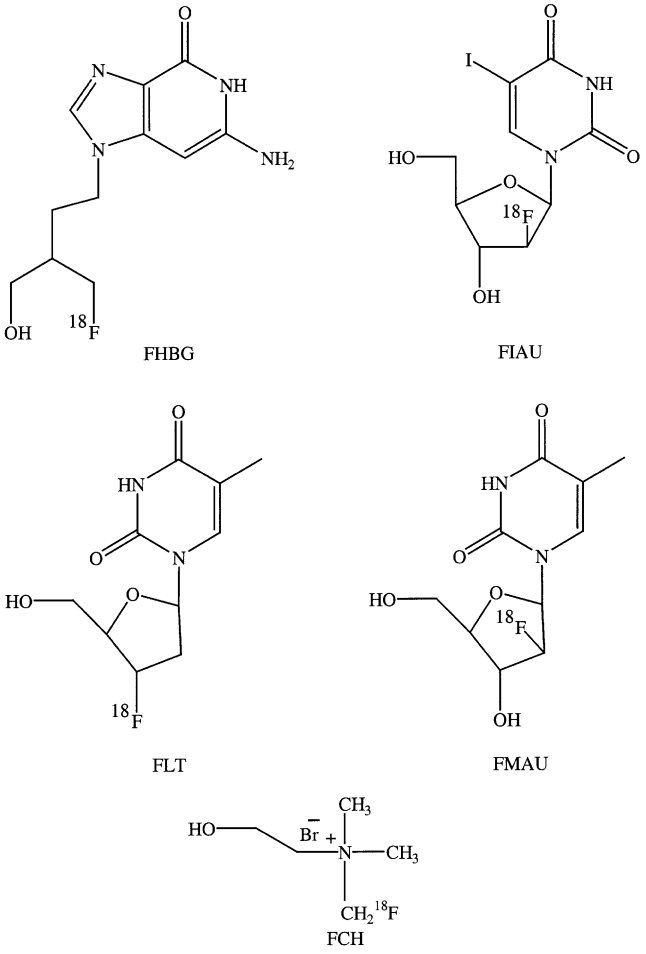

Figure 2. Structures of several nucleoside analogs and fluorocholine.

lular trapping of the radiopharmaceuticals. When prepared at high-specific activity, each has shown promise as a measure of cell and tumor proliferation (31). While further studies are needed for validation, a recent clinical trial shows excellent correlation between FLT standard uptake values and independent assessment of proliferation by Ki-67 immunostaining of lung nodules (34).

Choline Kinase

Many cancers show a high content of phosphorylcholine by ^{31}P nuclear magnetic resonance, whereas normal tissues show low or nondetectable levels (35). Choline is thought to be transported into cells by an active transporter mechanism (36), and phosphorylcholine, a product of choline kinase, is the first intermediate in the incorporation and trapping of choline into the phospholipid pool (37). Based on this biochemical pathway and the observation that choline uptake and phosphorylation are increased in tumor cells, choline has been developed as a PET tracer for tumor imaging (37). Several analogs have been reported, including [^{11}C]choline (38), [^{18}F]fluoroethylcholine (37), and [^{18}F]fluoromethylcholine (FCH) (39) (Fig. 2). A wide range of cancers have been visualized with radiolabeled choline analogs, such as tumors of the brain, lung, head and neck, colon, and bladder, but most recent studies have focused on imaging primary prostate cancer and metastasis. Because [^{18}F]fluoroethylcholine appears to have more rapid accumulation of radioactivity into the urinary bladder than [^{18}F]FCH, there may be advantages to the use of [^{18}F]FCH for PET imaging of primary prostate cancer (39). At least in part due to reduced bladder activity, PET studies in humans have shown that [^{18}F]FCH is better than FDG for detecting primary and metastatic prostate cancer (40).

Somatostatin and Other Peptide Receptors

Somatostatin is a cyclic 14-amino acid peptide that regulates both endocrine and exocrine secretion through inhibition of the release of many hormones, such as growth hormone (GH), insulin, glucagon, gastrin, secretin, and vasoactive intestinal peptide (41–44). Biological activity is mediated by somatostatin receptors, members of the superfamily of G-coupled receptors with seven transmembrane-spanning domains. Five somatostatin receptor subtypes (SSTR1-5) have been cloned (45,46). Further diversity of these receptors is evident by subclassification of the *sstr2* gene into *sstr2A* and *sstr2B* based on the length and sequence of C-terminus amino acid residues (47). As with other G-coupled receptors, SSTR function is regulated by interactions with specific G protein family members and by receptor-mediated endocytosis and receptor recycling (42). Somatostatin receptors, while widely distributed throughout the body, have also been found to be expressed on many tumors of neuroendocrine origin, such as somatotrophic tumors of the anterior pituitary and pancreatic islet-cell tumors (48–50). In addition, cells and tumors not of neuroendocrine origin, such as lymphocytic subtypes, lymphomas, and breast cancer, also possess somatostatin receptors (51–53). Therefore, nonmetabolized SSTR-targeted radiolabeled peptides have been explored as a class of radiopharmaceuticals for molecular imaging of cancer.

Receptor-targeted peptides should possess several characteristics essential for their success in diagnostic applications: 1) the cognate receptors should be expressed in abundance and possess high affinity for a given amino acid sequence; 2) the natural ligand may bind with similar affinity to several receptor subtypes — it may be desirable for synthetic analogs to bind specific receptor subtypes overexpressed in cancer; 3) receptor-mediated endocytosis and peptide internalization is preferred, resulting in image stability over time; 4) peptide analogs and their bifunctional chelates should be stable in the presence of peptidases; 5) rapid clearance from nontarget tissues is necessary; and 6) low cross-reactivity to related receptors is required (high specificity). Below are discussed various peptide-based radiopharmaceuticals for imaging tumors.

The utility of somatostatin itself as a radiopharmaceutical is limited, primarily due to rapid proteolytic degradation of the peptide, leading to a short serum half-life of ~3 minutes. Therefore, imaging applications would need a continuous infusion of the native labeled peptide. Consequently, peptides that are capable of incorporating radionuclides and are resistant to proteolytic degradation have been synthesized for diagnostic

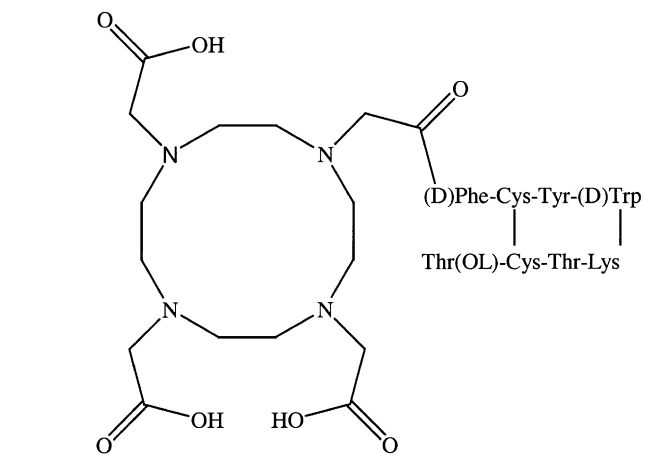

DOTA-Tyr^3-Octreotide

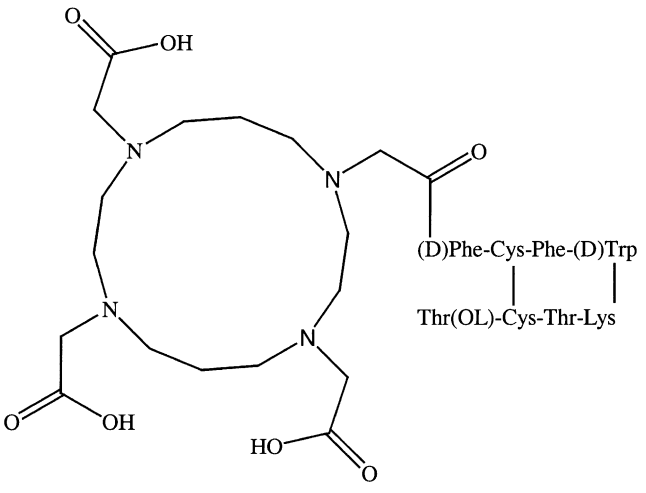

TETA-Octreotide

Figure 3. Structures of exemplary peptide-based receptor-targeted radiopharmaceuticals.

applications. The best-characterized SSTR-targeted agent is an ^{111}In-labeled analog of somatostatin comprising 8-amino acid residues commonly known as octreotide (54). Combined characteristics of stability under physiological conditions and efficient renal clearance (low background activity) (55) make this compound a versatile reagent to image tumors that express somatostatin receptors (55,56). In addition, other somatostatin analogs, including RC-160 and P829, have been labeled with a variety of radionuclides, including ^{99m}Tc (57–60), ^{64}Cu (61,62),^{68}Ga (63), ^{18}F (64), and ^{86}Y (65,66) for diagnostic molecular imaging. Animal imaging studies have also been reported with octreotide coupled to desferrioxamine-B (DFO) for incorporation of the radionuclides ^{68}Ga and ^{67}Ga (63,67). Furthermore, ^{68}Ga-DOTA-Tyr^3-octreotide, where DOTA = 1,4,7,10-tetraazacyclododecane-1,4,7,10-tetraacetic acid (^{68}Ga-DOTATOC) (Fig. 3) has been assessed for its potential as a PET radiopharmaceutical for imaging patients with meningiomas (68). Another bifunctional chelate that has been incorporated into octreotide is TETA (1,4,8,11-tetraazacyclotetradecane-1,4,8,11-tetraacetic acid) (61) (Fig. 3). The PET radiopharmaceutical ^{64}Cu-TETA-octreotide has been shown to possess high affinity for SSTR and efficient renal clearance (62).

Neurotensin (NT) is a 13-amino acid peptide originally isolated from calf hypothalamus (69) and bovine intestinal tissue (70). Like other neuropeptides, NT fulfills a dual function of both neurotransmitter/neuromodulator in the nervous system and local hormone in the periphery through interaction with receptors (71). For example, neurotensin receptors (NTRs) have been found to be expressed in a majority of pancreatic tumors (72,73). Three subtypes of NTRs have been cloned. NTR1 and NTR2 belong to the G protein-coupled receptor superfamily (74–76), whereas NTR3 is structurally different from NTR1 and NTR2 (77). Among these receptors, research activity in peptide-based receptor-targeted radiopharmaceuticals has primarily focused on NTR1 (78). Various nuclides such as ^{111}In, ^{201}Tl, and ^{99m}Tc have been incorporated into the active fragment of NT (known as NT(8–13)) through various strategies, including bifunctional chelates, such as diethylenetriamine pentaacetic acid (DTPA) (79), peptide-based chelators (80), and technetium-carbonyl complexes (81,82). In addition, PET radiopharmaceuticals have been obtained by incorporation of ^{18}F[fluoro benzoyl] into the NT(8–13) peptide (83).

Integrin $\alpha_v\beta_3$ is a transmembrane protein that affects tumor growth, invasion, and metastases. During angiogenesis, $\alpha_v\beta_3$ is upregulated on activated endothelial cells, making this integrin an important target of new tumor-specific therapies for cancer (84). $\alpha_v\beta_3$ recognizes a specific conformation of the tripeptide motif arginine-glycine-aspartic acid (RGD). To enable noninvasive imaging of $\alpha_v\beta_3$, researchers have developed radiolabeled cyclic peptides that contain the RGD motif (85). In animal models, high target-to-background accumulation of labeled RGD peptide has been observed with both SPECT and PET radiotracers. Potentially, PET imaging of $\alpha_v\beta_3$ can quantify receptor density at a tumor site to allow noninvasive monitoring of early treatment effects.

Other receptor-targeted peptide-based radiopharmaceuticals include bombesin (BN) analogs (DTPA-Pro^1,Tyr^4)BN(5–13) and its variants (86), and vasoactive intestinal peptide (VIP), a 28-amino acid peptide isolated from porcine intestine (87), appended to bifunctional chelators MAG_3 (N′-[N″[N‴(benzylthio)acetyl] glycyl]glycyl]glycine) with or without a lysine spacer. Labeled with ^{99m}Tc, the VIP analog TP3654 has been shown to image colorectal cancer that expresses VIP receptors in high density (88). Finally, ^{123}I-VIP has also been used to image patients with adenocarcinomas and endocrine tumors of gastrointestinal tracts (89). However, the difficulties of labeling with ^{123}I, limited availability of this isotope, and high background activity, especially in the thorax, may limit widespread utility of this agent.

Peptide-based radiopharmaceuticals also have been used for in vivo imaging of phosphatidylserine (PS), a lipid component of cell membranes. PS normally is confined to the inner leaflet of cell plasma membranes by an ATP-dependent translocase. During apoptosis, the translocase for PS is inactivated and a membrane

scramblase is activated, resulting in exposure of PS on the outer leaflet of the plasma membrane. Exposure of PS to the extracellular environment is the principal signal for recognition and phagocytosis of apoptotic cells (90). Because the endogenous protein annexin-V binds to PS with very high affinity (K_a = 7 nM) (91), binding of fluorescently labeled annexin-V is commonly used to detect apoptotic cells in vitro. Recently, annexin-V has been labeled with ^{99m}Tc to allow molecular imaging of cell death in vivo (92,93). In animal models of hepatic apoptosis induced by anti-Fas antibody, rejection of cardiac allografts, and chemotherapy of tumor xenografts, SPECT imaging showed that accumulation of ^{99m}Tc–annexin-V in sites of cell death increased by two- to sixfold above control values. ^{99m} Tc–annexin-V has been used clinically to noninvasively detect rejection of cardiac allografts, showing the feasibility of using this radiopharmaceutical to image exposure of PS (94). One important caveat for imaging with ^{99m}Tc–annexin-V is that binding to PS is not specific for apoptosis, because disruption of the plasma membrane during necrosis also exposes the radiopharmaceutical to PS that has not been scrambled to the external leaflet of the plasma membrane.

To utilize peptide radiopharmaceuticals as molecularly targeted neuroimaging agents, mechanisms must be developed to transport peptides across the blood-brain barrier (BBB). One strategy that has been successful in animal models exploits receptor-mediated transcytosis of transferrin receptors (TRs) across capillary endothelial cells at the BBB (95). Use was made of an engineered chimeric peptide that contains separate domains for binding to the epidermal growth factor receptor (EGFR) and TR. Binding to the TR mediates transfer of the chimeric peptide across the BBB, providing access of the radiopharmaceutical to EGFR expressed in an animal model of brain cancer. Binding of this peptide to tumor tissue was 20-fold greater than normal brain parenchyma (96), demonstrating the feasibility of using the transferrin receptor to deliver radiolabeled peptides to the central nervous system for molecular imaging.

Sodium/Iodide Symporter (NIS)

NIS is a membrane glycoprotein that uses the transmembrane sodium gradient maintained by the sodium/potassium ATPase to co-transport iodine and sodium into cells. Secondary active transport of iodine by NIS occurs in the thyroid gland, lactating breast epithelium, salivary glands, and gastric mucosa (97). Thus, these tissues concentrate radioactive isotopes of iodine (such as ^{123}I and ^{131}I) or ^{99m}Tc-pertechnetate, which has been used in clinical nuclear medicine for diagnosis and targeted therapy of thyroid gland pathology (98). NIS transport is maintained in thyroid malignancies, albeit at a decreased activity relative to normal thyroid tissue, enabling detection of recurrent and/or metastatic thyroid cancers as sites of enhanced accumulation of radiotracer (hot spots). While these imaging techniques are an integral part of management and therapy of patients with thyroid cancer, recent studies indicate that molecular imaging of NIS may have significance for therapy and detection of other cancers.

NIS has been used as a suicide gene for treatment of tumors in animal models. Boland et al used an adenoviral vector to transfer the NIS gene to tumor xenografts in mice. NIS functioned normally in these cells, as evidenced by specific accumulation of ^{123}I as detected by imaging and analysis of tumor specimens (99). A similar approach was used by Spitzweg et al to treat prostate tumor xenografts (100). Expression of NIS significantly enhanced uptake of ^{131}I and produced an 84% reduction in tumor volume. However, application of NIS as a suicide gene has been limited by lack of retention of radioactivity in nonthyroid tissues (101). Retention of iodine within heterologous tissues can be enhanced by co-expressing thyroperoxidase, the enzyme that catalyzes organification of iodine in thyroid (102). Thus, detecting and quantifying NIS function in vivo may become important in the future for monitoring this gene therapy approach to targeted radiotherapy of cancers.

Recent studies also suggest possible diagnostic and therapeutic applications of imaging NIS in breast cancer. In mouse models of breast adenocarcinoma, some tumors expressed functional NIS, as evidenced by specific accumulation of ^{99m}Tc-pertechnetate on both imaging studies and direct analysis of tumor specimens (98). Radiotracer did not accumulate in tumors that lack NIS or normal breast parenchyma. Immunohistochemistry showed expression of NIS in 80% of breast cancer specimens, although patients with breast cancer were not imaged in this study. Moon et al analyzed uptake of ^{99m}Tc-pertechnetate in patients with breast cancer and found accumulation of radiotracer in approximately 20% (103). In these patients, expression of NIS mRNA correlated with positive and negative uptake of ^{99m}Tc-pertechnetate. Although further studies are needed to validate these initial observations, the data suggest that molecular imaging of NIS function could become an important tool in detection and follow-up of primary and metastatic breast cancer.

Multidrug Resistance P-Glycoprotein

Emergence of multidrug resistance (MDR) is a major obstacle to successful chemotherapy of cancer. Several of the first characterized mechanisms of MDR include transporter-mediated resistance conferred by increased expression of the M_r 170,000 transmembrane glycoprotein, P-glycoprotein (Pgp), the product of the *MDR1* gene (104–108), and a related M_r 190,000 membrane glycoprotein, the MDR-associated protein (MRP1) (109,110). Pgp and MRP1 are members of the ATP-binding cassette (ABC) superfamily of membrane transport proteins (111) and confer resistance to an overlapping array of structurally and functionally unrelated toxic xenobiotics, natural product drugs, and, in the case of MRP1, conjugated compounds (112,113). Several other transporters have been shown to transport chemotherapeutic drugs and may be associated with MDR, including the lung resistance protein (LRP) (114); the breast cancer resistance protein (BCRP/MXR/ABCP), an ABC "half-transporter" (115–117); and MRP2-5 (111). Cells in culture exhibiting MDR by selection in cytotoxic drugs or transfection with these recombinant transporters generally show reduced net

drug accumulation and altered intracellular drug distribution.

MDR1 Pgp and related ABC transporters have been targets for cancer therapy on two fronts. First, reversal of MDR in tumor cells by nontoxic agents that block the transport activity of these ABC proteins has been an important target of pharmaceutical development (118). When co-administered with a cytotoxic agent, these inhibitors, known as MDR modulators, enhance net accumulation of cytotoxic compounds within the tumor cells. Several high-potency modulators discovered by targeted synthesis or combinatorial chemistry in combination with high-throughput screening are now in clinical trials (119–124). Second, transgenic expression of the *MDR1* gene has been explored for hematopoietic cell protection in the context of cancer chemotherapy (125–127), wherein Pgp could protect hematopoietic progenitor cells from chemotherapy-induced myelotoxicity. Hematopoietic cells transduced via retroviral-mediated transfer of the *MDR1* gene have shown preferential survival after treatment of the animal with MDR drugs (127), and recent pilot clinical data support the approach (128). For proper use of MDR modulators and for monitoring MDR gene therapy in chemotherapeutic protocols, identification of transporter-mediated resistance could guide the choice of agents and provide important prognostic information for cancer patients. Thus, noninvasive molecular imaging with a transport substrate serving as a surrogate marker of chemotherapeutic agents may identify those tumors and tissues in which ABC transporter proteins are expressed and active.

To achieve this goal, several gamma-emitting compounds have been synthesized, validated, and characterized as transport substrates for *MDR1* Pgp (129). One of the best characterized is *hexakis*(2-methoxyisobutyl isonitrile)^{99m}Tc(I) (^{99m}Tc-sestamibi) (Fig. 4), a widely available radiopharmaceutical that may enable scintigraphic analysis of MDR (130–134). The targeted synthesis and validation of several other single-photon radiopharmaceuticals for imaging MDR has been reported (11,135–141). Most of these radiopharmaceuticals are cationic and modestly hydrophobic, which is similar to many chemotherapeutic drugs in the MDR phenotype. For example, ^{99m}Tc-sestamibi accumulates within cells in response to the physiologically negative mitochondrial and plasma membrane potentials (131,142). However, functional *MDR1* Pgp mediates net outward transport of ^{99m}Tc-sestamibi from cells, reducing cellular accumulation of the radiopharmaceutical. Thus, cellular accumulation of ^{99m}Tc-sestamibi into drug-sensitive tumor cells is high and translates into a hot spot on scintigraphic images or a slow washout rate from a tumor focus. Conversely, expression of *MDR1* Pgp transports the tracer out of cells, thereby resulting in reduced net accumulation. This will be detected either as a "cold" tumor or as a rapid washout rate from a tumor focus or Pgp-expressing tissue (Fig. 5). Similar results are obtained with another widely available radiopharmaceutical, [1,2-*bis*{*bis*(2-ethoxyethyl)phosphino}ethane]$_2O_2$^{99m}Tc(V) (^{99m}Tc-tetrofosmin) (Fig. 4) (140), as well as with selected agents in preclinical development (139,141,143).

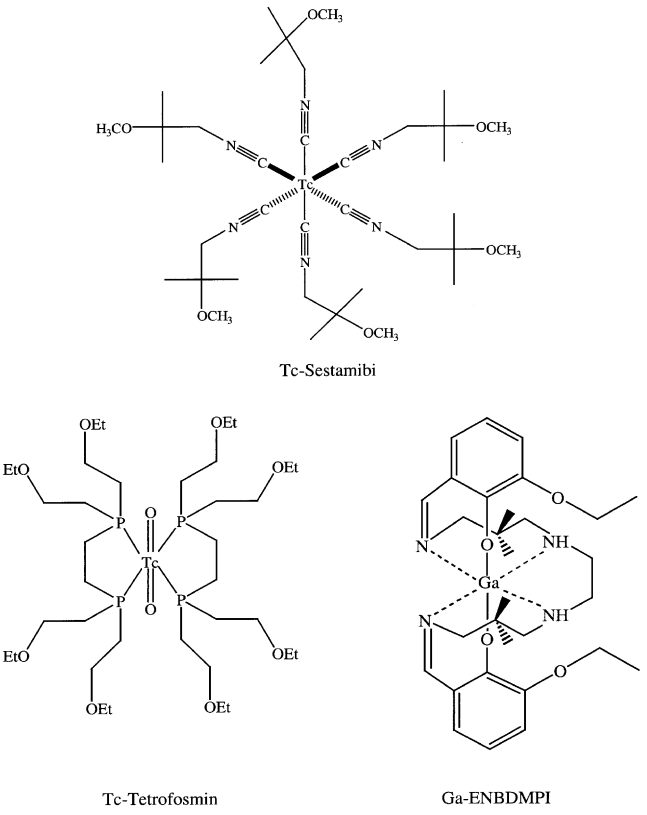

Figure 4. Structures of several radiotracers recognized as transport substrates by the *MDR1* Pgp.

In addition, several PET agents structurally based on MDR substrates or modulators and labeled with a conventional PET nuclide (^{11}C) have been characterized (144–146). Recently, MDR radiopharmaceuticals incorporating ^{18}F, the most widely used PET isotope, have been reported. One promising agent synthesized using this strategy, ^{18}F-paclitaxel, shows promise in preclinical models (147). In addition, radiopharmaceuticals containing nonconventional PET nuclides, such as ^{64}Cu, have been synthesized and their ability to probe transport activity of *MDR1* Pgp assessed (148–151). However, currently evaluated members of these classes of ^{64}Cu-based PET radiopharmaceuticals show rather modest Pgp-targeting properties. Exploiting the positron emissions of ^{94m}Tc, ^{94m}Tc-sestamibi has been synthesized and evaluated as a PET MDR agent (152). This approach has the advantage that all the biochemical and clinical validation studies already published for ^{99m}Tc-sestamibi apply directly to ^{94m}Tc-sestamibi. Other targeted metallo-radiopharmaceuticals have been obtained belonging to a class of multidentate ligands that possess an N_4O_2 donor core for incorporation of the PET nuclide ^{68}Ga. Selected compounds in this class have demonstrated high net cellular accumulation differences between wild-type (WT) and Pgp-expressing cells (143). Like ^{99m}Tc-sestamibi, these $^{67/68}$Ga-radiopharmaceuticals demonstrate enhanced accumulation in the presence of *MDR1*-specific modulators such as GF120918 and PSC 833 (valspodar). Of note, quantitative pharmacokinetic analysis was performed with one Ga complex ($^{67/68}$Ga-ENBDMPI) (Fig. 4) in WT and *mdr1a/1b* (–/–) gene disrupted knockout (KO) mice. Compared with WT

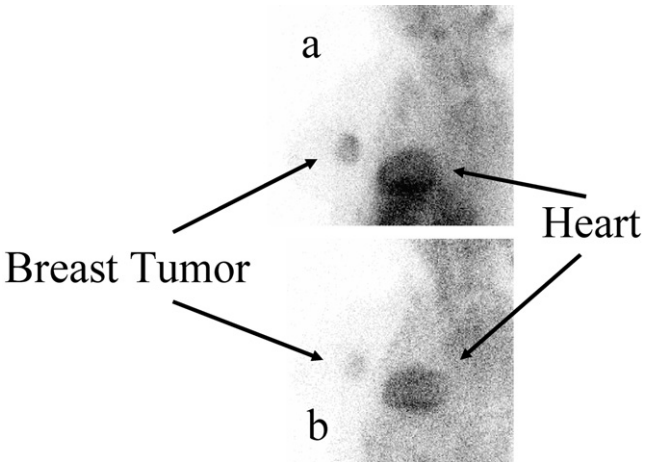

Figure 5. Molecular imaging of *MDR1* Pgp transport activity in vivo with the lipophilic cation ^{99m}Tc-sestamibi. Cellular accumulation of the agent into drug-sensitive tumor cells will be high in response to the inwardly directed driving forces of the inside-negative plasma membrane and mitochondrial potentials. This will translate to a hot spot on scintigraphic imaging or a slow washout rate from a tumor focus. Conversely, expression of the *MDR1* Pgp transporter on the cell surface will outwardly transport the tracer, thereby resulting in reduced net accumulation or a rapid washout rate from a tumor focus. **a:** Oblique lateral thoracic planar image obtained 1 hour after intravenous injection of ^{99m}Tc-sestamibi shows tracer uptake in a primary breast tumor. **b:** Significant tumor clearance of the radiotracer has occurred by 4 hours, consistent with MDR. Note efflux of tracer from liver (inferior to the heart), a result of prompt Pgp-mediated clearance. The heart, a Pgp-negative tissue, serves as an internal control and shows little difference in retention of activity. Images courtesy of F. Dehdashti, MD, Division of Nuclear Medicine, Mallinckrodt Institute of Radiology, St. Louis, Missouri.

control, ^{67}Ga-ENBDMPI demonstrated enhanced penetration into brain tissue and delayed clearance from livers of KO mice, directly demonstrating by imaging the functional loss of Pgp expression in brain capillary endothelial cells and bile canalicular surfaces of hepatocytes.

Several clinical studies have shown the feasibility of interrogating Pgp transport activity in vivo, with imaging cameras commonly available in nuclear medicine facilities (153–161). In general, ^{99m}Tc-sestamibi pharmacokinetic data are extracted from tumor images over time and correlated with immunohistochemical assessment of Pgp expression in the tumor specimen. For example, Del Vecchio et al determined rates of efflux of ^{99m}Tc-sestamibi in 30 patients with untreated breast cancer (153). Dynamic imaging of the primary tumor was performed for 4 hours following injection of ^{99m}Tc-sestamibi, and tumor specimens were obtained for quantitative autoradiography of Pgp. Rates of efflux of ^{99m}Tc-sestamibi were 2.7-fold greater in tumors overexpressing *MDR1* Pgp than in tumors that expressed Pgp at a level comparable to benign breast lesions. Estimates of sensitivity and specificity for in vivo detection of *MDR1* Pgp using ^{99m}Tc-sestamibi were 80% and 95%, respectively. From these data, the authors concluded that efflux rate constants of ^{99m}Tc-sestamibi may be used for noninvasive identification of *MDR1* Pgp in breast cancer.

Several additional clinical studies have examined the relationship between tumor retention of ^{99m}Tc complexes and MDR (160–163). Analysis of washout rates by comparing early (<30 minutes) and delayed (180–240 minutes) SPECT and planar images have shown a strong inverse correlation between tumor-to-background ratios and levels of Pgp expression. The relation between therapeutic response and tumor retention of tracer was also analyzed in some studies and showed that most tumors with high tracer retention exhibited a favorable response to chemotherapy, whereas most tumors with low tracer retention did not respond to chemotherapy. These investigators have concluded that ^{99m}Tc-sestamibi and ^{99m}Tc-tetrofosmin are useful tools in vivo for prediction of MDR in a variety of cancers.

Early uptake, delayed uptake, and washout rates of ^{99m}Tc-sestamibi also have been obtained for correlation with *MDR1* Pgp, MRP1, and LRP protein expression determined by immunohistochemistry and *MDR1* Pgp, MRP1, and LRP mRNA levels determined by real-time reverse-transcription polymerase chain reaction (164). These investigators found that increased levels of Pgp expression correlated with a low accumulation of ^{99m}Tc-sestamibi on delayed scans and a high washout rate of ^{99m}Tc-sestamibi. Interestingly, neither MRP1 nor LRP expression on the level of either protein or mRNA correlated significantly with tumor accumulation or efflux of ^{99m}Tc-sestamibi in lung cancer. Thus, although ^{99m}Tc-sestamibi has been shown to modestly cross-react with MRP1 using cells in culture under ideal laboratory conditions (140,165), unlike the case with *MDR1* Pgp, this lower level of MRP1 transport activity cannot be detected in patients in vivo. As a practical consequence, when used in patients, ^{99m}Tc-sestamibi may be specific for detection of *MDR1* Pgp transport activity in vivo.

Furthermore, in addition to the in vitro and animal laboratory studies cited above, clinical blockade of Pgp-mediated extrusion of ^{99m}Tc-sestamibi from tissues and tumors of patients has been imaged following treatment with highly selective and potent Pgp modulators such as PSC 833 (valspodar), VX-710 (biricodar), and XR-9576 (tariquidar) (111,155,156,166). A two-step protocol for imaging MDR reversal in patients is under evaluation, which may provide a noninvasive method to determine the effectiveness of MDR modulation. After baseline imaging, administration of a potent modulating agent and reinjection of the tracer is performed. Those tissues or tumors showing higher accumulation of the tracer and/or reduced washout rates would indicate specific blockade of *MDR1* Pgp. Thus, these radiopharmaceuticals enable noninvasive mapping of specific transport events in vivo and provide a basis for further exploration of targeted molecular imaging of Pgp in cancer and gene therapy.

Cell Membrane Permeant Peptides

Peptide-based imaging agents are desired for molecular imaging applications because of their potential for specific detection of a target and the availability of well-characterized moieties for stable chelation of isotopes such as ^{99m}Tc. Fragments of antibodies (single chain fragments, diabodies, or minibodies) (167) and small

peptides (3,8) have been used successfully to detect cell surface proteins such as carcinoembryonic antigen or SSTR2 receptors. However, peptides and small proteins typically have poor permeability through the plasma membrane of cells, thus limiting molecular targets to proteins that contain extracellular domains. Imaging receptors on the cell surface also potentially limits detection of the tracer, because signal amplification through transport into cells or enzymatic activity does not occur.

Investigators have identified several small proteins and peptides that permeate plasma membranes of intact cells. Included among these peptides are the third helix of the homeodomain of Antennapedia (168) and viral proteins such as herpes simplex virus VP22 (169), human immunodeficiency virus type 1 (HIV-1) Rev protein (170), and the basic domain of HIV-1 Tat protein (171,172). The mechanism through which these peptides enter cells remains uncertain, although it does not appear to depend on known mechanisms of receptor-mediated endocytosis. Not only do the peptides themselves transduce into cells, but they also can mediate entry of coupled peptides and full-length proteins (169,172,173), fluorophores (174), and derivatized superparamagnetic iron oxide particles (175).

We have shown that peptides based on the basic domain of Tat and an attached chelator for metals can be used to deliver ^{99m}Tc into cells in vitro (176,177). These peptides quickly (<2 minutes) accumulate and concentrate within cells in culture while maintaining stable chelation of the radioisotope. In addition, conjugation of the peptide with fluorescein can directly reveal the intracellular localization of the peptide when cells are viewed under a fluorescence microscope. Washout of Tat peptides from cells also demonstrates similar rapid kinetics. When injected into mice, radiolabeled Tat peptides distribute throughout the body, reaching peak accumulation in organs and tissues within minutes. The peptide subsequently clears primarily through the kidneys during the first hour after injection. Thus, the pharmacokinetic data suggest that Tat peptides may be useful agents for imaging.

However, to make these peptides useful for molecular imaging, targeting moieties need to be engineered into the peptide. Thus, a peptide sequence specifically recognized by an intracellular enzyme could be inserted between the transduction domain and the peptide chelator for the radioisotope. Using this approach, intracellular trapping of the radiotracer would occur only in cells that have the desired enzymatic activity, similar to accumulation of phosphorylated FDG in cells that overexpress hexokinase. This strategy for selective targeting with Tat peptides has been exploited previously by incorporating the recognition sequence for HIV protease between the Tat domain and a precursor form of caspase 3, an enzyme that is activated in apoptotic cell death (178). Only cells infected with HIV cleave the Tat peptide and release functional caspase 3, resulting in specific killing of these cells. Tat peptides also have been shown to transduce a functional enzyme (β-galactosidase) into cells in living mice (179), implying that other reporter genes for oncologic molecular imaging could be transduced in vivo.

IMAGING EXOGENOUS GENE EXPRESSION: REPORTER GENE CONCEPT

Reporter genes are commonly used in molecular biology to monitor expression and/or repression of a gene of interest. Typical reporter genes consist of a chimeric gene linking an endogenous or exogenous enhancer or promoter to a gene encoding an enzyme (luciferase or β-galactosidase) or fluorophore (green fluorescent protein (GFP)). In all cases, the reporter must be introduced into the target cell or tissue, using a variety of methods, including transfection of plasmid DNA, transduction with viral vectors, or incorporation into the DNA of genetically engineered animals. The reporter gene can then be used to detect activation of the promoter and/or enhancer of interest, which is inferred to duplicate expression of the endogenous gene(s) controlled by the same promoter elements. Ideally, the magnitude and time course of reporter gene activity should parallel the strength and duration of expression of the endogenous target gene.

For detection of gene expression and regulation in vivo with PET, researchers have had to develop and characterize new reporter systems. Most studies have used either heterologous enzymes such as herpes simplex virus-1 TK (HSV1-TK) or receptors such as dopamine-2 (180,181) or SSTR2 (182,183). As compared with direct imaging of small quantities of mRNA, these systems have the potential to provide signal amplification at two biological levels and thereby increase sensitivity for detecting and localizing gene expression. First, a single mRNA transcript is translated into many copies of a receptor or enzyme. Second, each molecule of an enzyme can catalyze intracellular trapping of a large number of reporter probe molecules, thus theoretically providing a greater signal compared to a receptor system that binds a single reporter ligand at a time. However, enzyme systems as well as receptors have been used successfully for molecular imaging of gene expression (180,181). In addition, while conventional promoter-enhancer elements often are engineered directly upstream of the reporter gene of interest, so-called cis-acting systems, other variants of reporter systems useful for imaging are trans-acting systems. Herein, the first promoter-enhancer drives expression of an intermediate transcription factor that then binds a second promoter-enhancer element to drive expression of a target reporter gene (184). This approach provides the potential for trans-activating systems to amplify signals arising from weak primary promoters as the intermediate transcription factor can repetitively trans-activate multiple target promoters. These and other reporter strategies enable direct imaging of exogenous gene expression as well as indirect imaging of endogenous gene expression via use of endogenous promoters driving reporter constructs. Another fundamental advantage of any reporter gene/reporter probe system is that once validated, the reporter gene can theoretically be cloned into an appropriate vector and any gene of interest can be interrogated with the same validated reporter probe. For PET, this eliminates the constraints inherent to traditional routes of synthesizing, labeling, and validating a new and different radioligand for every new receptor or protein of interest.

Dopamine-2 Receptor

The dopamine-2 receptor (D2R) is expressed in the plasma membrane of cells, primarily in the striatum of the brain and the pituitary gland. Several different ligands for PET or SPECT imaging of D2R have been validated, including 3-(2′-^{18}F-fluorethyl)spiperone (^{18}F-FESP) and ^{123}I-iodobenzamine. Investigators have shown that expression of D2R can be detected in living mice, using either a replication-incompetent adenovirus that targets the reporter gene to liver or an implanted tumor that stably expresses D2R (185). In both models, binding of ^{18}F-FESP to D2R as measured by PET in vivo has a high correlation with in vitro assays of D2R mRNA expression, amount of protein, and ligand-receptor binding. By PET imaging, significantly more accumulation of ^{18}F-FESP was measured in tumors transfected with D2R than tumors without this receptor. D2R also has been used in conjunction with HSV1-TK to quantify relative gene expression from the first and second genes in bicistronic transcripts, showing the feasibility of using PET to monitor expression of a therapeutic gene in vivo (186).

One limitation of using D2R as a reporter protein is that signaling through endogenous ligands can perturb the underlying biology of the cell or tissue of interest. To reduce this potential problem, Liang et al recently used a mutant D2R as a reporter protein for molecular imaging (181). Point mutations within the receptor uncoupled ligand binding from inhibition of the second messenger molecule cyclic adenosine monophosphate in cells. Importantly, WT and mutant D2R receptors bound equivalent amounts of ^{18}F-FESP in living mice, validating use of the mutant D2R as a reporter protein for molecular imaging.

Somatostatin-2 Receptor

Receptor-targeted peptide-based radiopharmaceuticals have been used to noninvasively monitor gene transfer using SSTR2. In a tumor model, using a replication-incompetent adenoviral vector encoding the human SSTR2 (Ad5-CMVhSSTR2), P829, a somatostatin receptor-avid peptide, was used to image expression of the hSSTR2 reporter (182). The studies demonstrated the potential of imaging the binding of a ^{99m}Tc-labeled peptide to the reporter receptor after in vivo gene transfer to the tumor cells. In addition, using a similar approach, adenovirus-mediated gene transfer to ovarian cancer xenografts has been imaged with a technetium-labeled peptide radiopharmaceutical, ^{99m}Tc-P2045 (187).

HSV1-TK and Cytosine Deaminase

Viral or bacterial enzymes that convert a prodrug into a toxic metabolite originally were investigated for use as suicide genes in therapy of cancer. Two of the most frequently used enzymes for therapeutic applications, cytosine deaminase (CD) from *Escherichia coli* and TK from HSV1, also have been used for molecular imaging of gene expression. CD, an enzyme that is absent in mammalian cells, converts cytosine to uracil; thus, only cells that express the transgene convert 5-fluorocytosine to the cytotoxic 5-fluorouracil. However, imaging of CD with radiotracers has been limited by slow uptake of 5-fluorocytosine and rapid diffusion of 5-fluorouracil out of cells (188). Conversely, HSV1-TK has been used extensively as a PET reporter for gene expression in vivo and will be reviewed more fully below.

The underlying principle for use of HSV1-TK in both therapeutic and imaging applications is manifest in the broad substrate specificity of HSV1-TK activity relative to endogenous TK, enabling robust phosphorylation of nucleoside analogs, such as ganciclovir, compared with endogenous TK normally present in mammalian cells. Following active transport of a nucleoside analog across the cell membrane, the agent is selectively phosphorylated only by viral TK. The monophosphorylated nucleoside is trapped within cells and subsequently converted to a nucleoside triphosphate. Approximately 50% of cell-associated nucleoside is converted to the triphosphate form and incorporated into DNA within 1 hour (189), where it acts to terminate DNA synthesis. These metabolic steps result in trapping of nucleoside analogs like ganciclovir selectively within cells that express HSV1-TK. In the absence of the viral thymidine analogs, nucleoside analogs are not phosphorylated by native enzymes and do not accumulate within cells. In pharmacological doses, incorporation of nucleoside analogs into DNA causes cell death. However, tracer amounts of radiolabeled nucleoside analogs can be trapped inside cells without causing toxicity, perhaps mediated in part by contributions of DNA repair enzymes (190), thus enabling repetitive imaging of HSV1-TK activity with SPECT or PET.

Use of radiolabeled nucleoside analogs to localize expression of HSV1-TK in living animals first was reported almost two decades ago by Saito et al (191,192). These authors administered FMAU to rats infected with HSV-1 and then used selective trapping of the drug to quantify and map sites of viral infection by autoradiography of brain sections. Accumulation of FMAU was correlated highly with sites of focal infection, as determined by immunoperoxidase staining for viral antigens. The authors also proposed that appropriately labeled nucleoside analogs could be used for clinical imaging of TK activity.

Since these initial reports, several different technical innovations and improvements have been made to enable imaging of HSV1-TK activity in vivo. Radiolabeled nucleoside analogs appropriate for in vivo detection of HSV1-TK by SPECT or PET have been developed and characterized, including uracil nucleoside derivatives, such as 5-iodo-2′-fluoro-2′-deoxy-1-β-D-arabinofuranosyl-5-iodouracil (FIAU) (Fig. 2) labeled with ^{124}I or ^{131}I, and derivatives of acycloguanosine, such as 8-[^{18}F]fluoro-9-[(2-hydroxy-1-(hydroxymethyl)ethoxy)-methyl]guanine (8-[^{18}F]-fluoroganciclovir; [^{18}F]FGCV), 9-[(3-[^{18}F]fluoro-1-hydroxy-2-propoxy)methyl]guanine ([^{18}F]FHPG), or 9-(4-[^{18}F]fluoro-3-hydroxymethylbutyl)-guanine ([^{18}F]FHBG) (193–195) (Fig. 2). To enable imaging of gene expression and other biologic processes in small animals such as mice, the development of microPET has been a significant advance in technology (Fig. 6). The first-generation microPET scanner has a volumetric resolution of approximately 2 mm^3 (196), allowing imaging of reporter gene activity at the level of an organ or tissue (197). Scanners that perform both PET

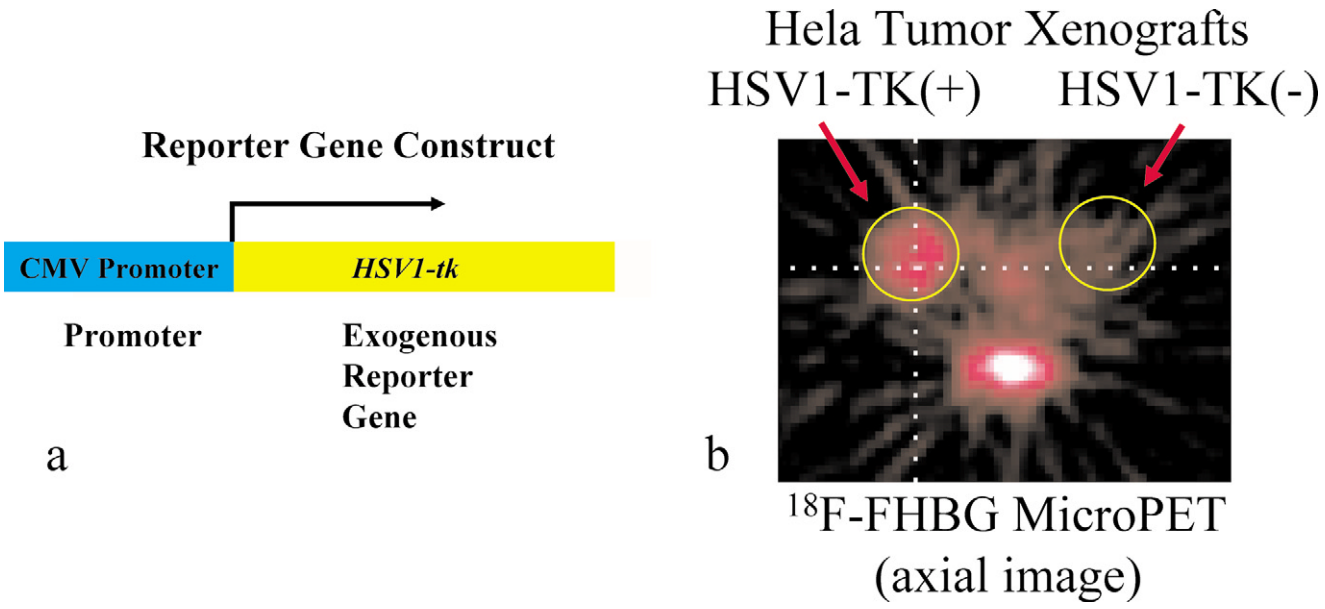

Figure 6. Molecular imaging of HSV1-TK with [^{18}F]-FHBG and microPET. **a:** Hela tumor cells were stably transfected with a reporter construct comprising the constitutive (always-on) cytomegalovirus (CMV) promoter driving the HSV1-TK gene. **b:** Hela cells expressing HSV1-TK (+) or control vector cells (–) were grown as tumor xenografts for ~1 week on the flanks of nude mice. One hour after intravenous injection of [^{18}F]-FHBG, transaxial microPET images through the lower abdomen and flanks show uptake of the tracer in the HSV1-TK (+)-expressing tumor.

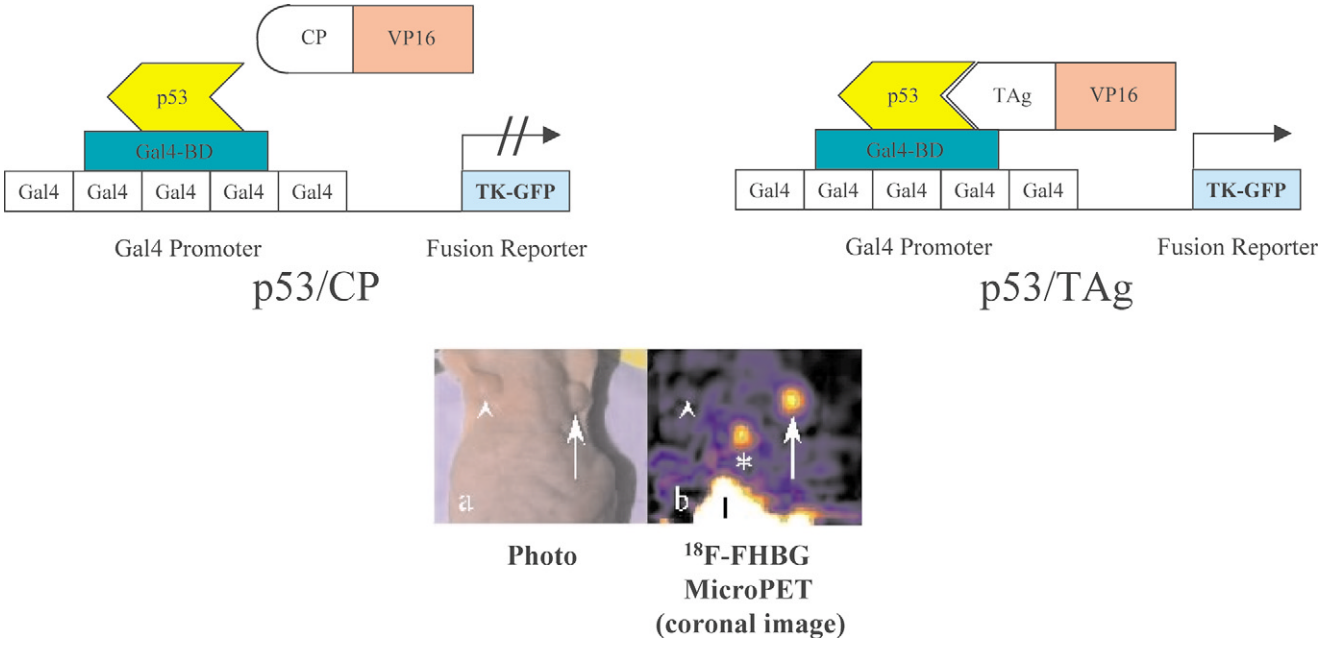

Figure 7. Molecular imaging of protein-protein interactions in vivo using microPET and reporter genes. The binding of one protein to another protein within cells regulates how cells divide, sends signals from the cell exterior to the cell interior, and mediates when and how cells move, grow, and die. Noninvasive imaging of these protein-protein interactions in vivo will provide a broad-based tool for researchers to integrate existing knowledge of protein interactions within the complex physiological context of living animals and also enable the study of drugs that target these interactions. The tumor suppressor protein p53 and a viral protein known as large TAg, two interacting proteins known to be involved in transforming normal cells into cancer, are each fused to different domains of a transcription factor. Both portions of the transcription factor are required to activate the PET reporter gene (HSV1-TK-GFP), but only one domain (Gal4BD) can bind on its own to specific DNA sequences that regulate activation of the reporter. However, when p53 and TAg proteins interact, the second domain (VP16) is now properly assembled, thereby switching on the reporter gene (upper right). The activated reporter can be detected by microPET imaging of living mice using the positron-emitting radiopharmaceutical [^{18}F]-FHBG. In contrast, when the VP16 activation domain is fused to a noninteracting protein (in this case, polyoma virus coat protein (CP)), the reporter gene cannot be activated (upper left). Photograph of the anterior thorax of a mouse with axillary xenograft tumors of Hela cells containing noninteracting p53-CP proteins (arrowhead) and interacting p53-TAg proteins (large arrow) (bottom, **a**). Coronal microPET image of the same mouse showing accumulation of [^{18}F]-FHBG only in the tumor expressing the interacting p53-TAg proteins (large arrow) (bottom, **b**). Asterisk denotes radiotracer in the gallbladder. Intestinal activity (l) from normal hepatobiliary clearance of the radiotracer is observed in the lower portion of the image. Modified from Luker et al (205).

and MRI have been developed for humans (198), allowing co-registration of functional PET images with anatomic localization of MRI. Combined scanners for microPET and CT or MR are under development and will provide similar benefits for molecular imaging in small animals.

To introduce HSV1-TK into animals for imaging, investigators have either transfected tumor cells with HSV1-TK in vitro, and subsequently implanted these cells into mice to form tumors, or delivered the reporter gene into liver via adenoviral vectors (189,199–201). Initial imaging studies with HSV1-TK used heterologous viral promoters, such as promoters of early genes in cytomegalovirus, Simian virus 40 (SV40), or Rous sarcoma virus, to drive expression of the reporter. These promoters provide constitutive, high-level amounts of enzyme that likely exceed expression driven by most endogenous mammalian promoters. More recently, investigators have shown the feasibility of imaging constitutive human promoters, such as elongation factor 1α (202), or promoters regulated by endogenous transcription factors, such as p53 or nuclear factor of activated T cells (203,204). In another recent advancement, protein-protein interactions were imaged in vivo by microPET and fluorescence imaging using an engineered fusion reporter gene comprising a mutant HSV1-TK and GFP for readout of a tetracycline-inducible two-hybrid system in vivo (205) (Fig. 7). Although a variety of methods have been used to investigate protein interactions in vitro and in cultured cells, none can analyze these interactions in intact, living animals. Using microPET, interactions between p53 tumor suppressor and the large T antigen (TAg) of SV40 were quantitatively visualized in tumor xenografts of Hela cells stably transfected with the imaging constructs. Protein-protein interactions control transcription, cell division, and cell proliferation as well as mediate signal transduction, oncogenic transformation, and regulation of cell death. Imaging protein binding partners in vivo will enable functional proteomics in whole animals and provide a molecular imaging tool for screening compounds targeted to specific protein-protein interactions in living animals.

Transgenic mice that use HSV1-TK as a reporter for upregulation or deletion of a specific gene also are in development. In one recent report, a transgenic mouse was engineered in which the endogenous albumin promoter drove expression of HSV1-TK primarily in the liver (206). [^{18}F]FHBG uptake in the liver was shown to correlate with changes in normalized albumin mRNA in response to the protein content of an experimental diet fed to the mice (207). These data suggested that PET reporter genes can indirectly monitor endogenous promoter activity in vivo. Progress in these areas of research will increase greatly the number and types of biological hypotheses that can be addressed by molecular imaging of gene expression in vivo with PET and SPECT.

REFERENCES

1. Pennisi E. Human genome: finally, the book of life and instructions for navigating it. Science 2000;288:2304–2307.
2. Tavitian B, Terrazzino S, Kuhnast B, et al. In vivo imaging of oligonucleotides with positron emission tomography. Nat Med 1998;4:467–471.
3. Krenning E, Kwekkeboom D, Bakker W, et al. Somatostatin receptor scintigraphy with [In-111-DTPA-D-Phe] and [I123-Tyr]-octreotide: the Rotterdam experience with more than 1000 patients. Eur J Nucl Med 1993;20:716–731.
4. Lister-James J, Vallabhajosula S, Moyer B, et al. Pre-clinical evaluation of technetium-99m platelet receptor-binding peptide. J Nucl Med 1997;38:105–111.
5. Perlmutter M, Slater S. Which nodular goiters should be removed? N Engl J Med 1956;255:61–71.
6. Luker GD, Piwnica-Worms D. Beyond the genome: molecular imaging *in vivo* with PET and SPECT. Acad Radiol 2001;8:4–14.
7. Hom R, Katzenellenbogen J. Technetium-99m-labeled receptor-specific small-molecule radiopharmaceuticals: recent developments and encouraging results. Nucl Med Biol 1997;24:485–498.
8. Liu S, Edwards D. ^{99m}Tc-labeled small peptides as diagnostic radiopharmaceuticals. Chem Rev 1999;99:2235–2268.
9. Anderson C, Welch M. Radiometal-labeled agents (non-technetium) for diagnostic imaging. Chem Rev 1999;99:2219–2234.
10. Volkert W, Hoffman T. Therapeutic radiopharmaceuticals. Chem Rev 1999;99:2269–2292.
11. Sharma V, Piwnica-Worms D. Metal complexes for therapy and diagnosis of drug resistance. Chem Rev 1999;99:2545–2560.
12. Eckelman W, Frank J, Brechbiel M. Theory and practice of imaging saturable binding sites. Invest Radiol 2002;37:101–106.
13. Grasby P. Imaging the neurochemical brain in health and disease. Clin Med 2002;2:67–73.
14. Piwnica-Worms D, Luker G, Anderson C, et al. Molecular imaging in oncology. In: Feinendegen LE, Shreeve WW, editors. Molecular nuclear medicine: the challenge from the human genome. Lansberg, Germany: Ecomed Publ., in press.
15. Warburg O. The metabolism of tumors. New York: Richard R. Smith, Inc.; 1931. p 1–129.
16. Brown R, Wahl R. Overexpression of Glut-1 glucose transporter in human breast cancer. An immunohistochemical study. Cancer 1993;72:2979–2985.
17. Younes M, Lechago L, Somoano J, et al. Wide expression of the human erythrocyte glucose transporter Glut 1 in human cancers. Cancer Res 1996;56:1164–1167.
18. Clavo A, Brown R, Wahl R. 2-fluoro-2-deoxy-D-glucose (FDG) uptake into human cancer cell lines is increased by hypoxia. J Nucl Med 1995;36:1625–1632.
19. Brown R, Leung J, Fisher S. Intratumoral distribution of tritiated fluorodeoxyglucose in breast carcinoma: correlation between Glut-1 expression and FDG uptake. J Nucl Med 1996;37:1042–1047.
20. Kubota K, Kubota R, Yamada S. FDG accumulation in tumor tissue. J Nucl Med 1993;34:419–421.
21. Aloj L, Caraco C, Jagoda E, et al. Glut-1 and hexokinase expression: relationship with 2-fluoro-2-deoxy-D-glucose uptake in A431 and T47D cells in culture. Cancer Res 1999;59:4709–4714.
22. Mochizuki T, Tsukamoto E, Kuge Y, et al. FDG uptake and glucose transporter subtype expressions in experimental tumor and inflammation models. J Nucl Med 2001;42:1551–1555.
23. Hoekstra C, Paglianiti I, Hoekstra O, et al. Monitoring response to therapy in cancer using [18F]-2-fluoro-2-deoxy-D-glucose and positron emission tomography: an overview of different analytical methods. Eur J Nucl Med 2000;27:731–743.
24. Larson S, Grunbaum Z, Rasey J. Positron imaging feasibility studies: selective tumor concentration of 3H-thymidine, 3H-uridine, and 14C-2-deoxyglucose. Radiology 1980;134:771–773.
25. Wahl R, Hutchins G, Buchsbaum D, et al. 18F-2-deoxy-2-fluoro-d-glucose (FDG) uptake into human tumor xenografts: feasibility studies for cancer imaging with PET. Cancer 1991;67:1544–1550.
26. Wahl R, Zasadny K, Helvie M, et al. Metabolic monitoring of breast cancer chemohormonotherapy using positron emission tomography (PET): initial evaluation. J Clin Oncol 1993;11:2101–2111.
27. Evan G, Vousden K. Proliferation, cell cycle and apoptosis in cancer. Nature 2001;411:342–348.
28. Christman D, Crawford E, Friedkin M, et al. Detection of DNA synthesis in intact organisms with positron-emitting methyl-[C-11]-thymidine. Proc Natl Acad Sci U S A 1972;69:988–992.
29. Vander Borght T, Labar D, Pauwels S, et al. Production of [2-C-11]thymidine for quantification of cellular proliferation with PET. Appl Radiat Isot 1991;42:103–104.

30. Conti P, Alauddin M, Fissekis J, et al. Synthesis of 2′-fluoro-5-[C-11]-methyl-1-beta-D-arabinofuranosyluricil ([C-11]-FMAU): a potential nucleoside analog for in vivo study of cellular proliferation with PET. Nucl Med Biol 1995;22:783–789.
31. Krohn K, Mankoff D, Eary J. Imaging cellular proliferation as a measure of response to therapy. J Clin Pharmacol 2001;41:96S–103S.
32. Shields A, Grierson J, Dohmen B, et al. Imaging proliferation in vivo with [F-18]FLT and positron emission tomography. Nature Med 1998;4:1334–1336.
33. Conti P, Allauddin M, Fissekis J, et al. Synthesis of [F-18]2-fluoro-5-methyl-1-beta-D-arabinofuranosyluricil ([F-18]FMAU). J Nucl Med 1999;40:83P.
34. Buck A, Schirrmeister H, Hetzel M, et al. 3-deoxy-3-[F-18]fluorothymidine-positron emission tomography for noninvasive assessment of proliferation in pulmonary nodules. Cancer Res 2002;62:3331–3334.
35. de Certaines J, Larsen V, Podo F, et al. In vivo 31P MRS of experimental tumours. NMR Biomed 1993;6:345–365.
36. Katz-Brull R, Seger D, Rivenson-Segal D, et al. Metabolic markers of breast cancer: enhanced choline metabolism and reduced choline-ether-phospholipid synthesis. Cancer Res 2002;62:1966–1970.
37. Hara T, Kosaka N, Kishi H. Development of F-18-fluoroethylchline for cancer imaging with PET: synthesis, biochemistry, and prostate cancer imaging. J Nucl Med 2002;43:187–199.
38. Hara T, Kosaka N, Shinoura N, et al. PET imaging of brain tumor with [methyl-^{11}C]choline. J Nucl Med 1997;38:842–847.
39. DeGrado T, Coleman R, Wang S, et al. Synthesis and evaluation of 18F-labeled choline as an oncologic tracer for positron emission tomography: initial findings in prostate cancer. Cancer Res 2001;61:110–117.
40. Price D, Coleman R, Liao R, et al. Comparison of [18 F]fluorocholine and [18 F]fluorodeoxyglucose for positron emission tomography of androgen dependent and androgen independent prostate cancer. J Urol 2002;168:273–280.
41. de-Herder W, Lamberts S. Somatostatin and somatostatin analogues: diagnostic and therapeutic uses. Curr Opin Oncol 2002;14:53–57.
42. Patel Y. Somatostatin and its receptor family. Front Neuroendocrinol 1999;20:157–198.
43. Reichlin S. Somatostatin (part 1). N Engl J Med 1983;309:1495–1501.
44. Reichlin S. Somatostatin (part 2). N Engl J Med 1983;309:1556–1563.
45. Bell G, Reisine T. Molecular biology of somatostatin receptors. Trends Neurosci 1993;16:34–38.
46. Bruns C, Weckbecker G, Raulf F. Molecular pharmacology of somatostatin receptor subtypes. In: Wiedenmann B, Kvol L, Arnold R, Riecken E, editors. Molecular and cell biological cell aspects of gastroenteropancreatic tumor disease. New York: NY Academy of Sciences; 1994. p 138–147.
47. Vanetti M, Kouba M, Wang X, et al. Cloning and novel expression of a novel mouse somatostatin receptor (SSTR2B). FEBS Lett 1992;311:290–294.
48. Patel Y, Amherdt M, Orci L. Quantitative electron microscopic autoradiography of insulin, glucagon, and somatostatic binding sites on islets. Science 1982;217:1155–1156.
49. Reubi J, Maurer R. Autoradiographic mapping of somatostatin receptors in the rat CNS and pituitary. Neuroscience 1985;15:1183–1193.
50. Reubi J, Kvols L, Waser B. Detection of somatostatin receptors in surgical and percutaneous needle biopsy samples of carcinoids and islet cell-carcinomas. Cancer Res 1990;50:5969–5977.
51. Sreedharan S, Kodama K, Peterson K, et al. Distinct subsets of somatostatin receptors on cultured human lymphocytes. J Biol Chem 1989;264:949–953.
52. Reubi J, Waser B, Foekens J. Somatostatin receptor incidence and distribution in breast cancer using receptor autoradiography: relationship to EGF receptors. Int J Cancer 1990;46:416–420.
53. Reubi J, Waser B, Vanhagen M. In vitro and in vivo detection of somatostatin receptors in human malignant lymphomas. Int J Cancer 1992;50:895–900.
54. Bakker WH, Albert R, Bruns C, et al. [111In-DTPA-D-Phe]-octreotide, a potential radiopharmaceutical for imaging of somatostatin receptor-positive tumors: synthesis, radiolabeling and in vitro validation. Life Sci 1991;49:1583–1591.
55. Krenning EP, Bakker WH, Kooij PPM, et al. Somatostatin receptor scintigraphy with indium-111-DTPA-D-Phe-1-octreotide in man: metabolism, dosimetry and comparison with iodine-123-Tyr-3-octreotide. J Nucl Med 1992;33:652–658.
56. Krenning EP, Kwekkeboom DJ, Bakker WH, et al. Somatostatin receptor scintigraphy with [^{111}In-DTPA-D-Phe^1]- and [^{123}I-Tyr^3]-octreotide: the Rotterdam experience with more than 1000 patients. Eur J Nucl Med 1993;20:716–731.
57. Pearson DA, Lister-James J, McBride WJ, et al. Somatostatin receptor-binding peptides labeled with technetium-99m: chemistry and initial biological studies. J Med Chem 1996;39:1361–1371.
58. Vallabhajosula S, Moyer BR, Lister-James J, et al. Preclinical evaluation of technetium-99m-labeled somatostatin receptor-binding peptides. J Nucl Med 1996;37:1016–1022.
59. Decristoforo C, Melendez-Alafort L, Sosabowski JK, et al. ^{99m}Tc-HYNIC-Tyr^3-octreotide for imaging somatostatin-receptor-positive tumors: preclinical evaluation and comparision with ^{111}In-octreotide. J Nucl Med 2000;41:1114–1119.
60. Bangard M, Behe M, Guhlke S, et al. Detection of somatostatin receptor-positive tumours using the new ^{99m}Tc-tricine-HYNIC-D-Phe^1-Tyr^3-octreotide: first results in patients and comparison with ^{111}In-DTPA-D-Phe^1-octreotide. Eur J Nucl Med 2000;27:628–637.
61. Anderson C, Pajeau T, Edwards W, et al. *In vitro* and *in vivo* evaluation of copper-64-octeotide conjugates. J Nucl Med 1995;36:2315–2325.
62. Anderson CJ, Dehdashti F, Cutler PD, et al. Copper-64-TETA-octreotide as a PET imaging agent for patients with neuroendocrine tumors. J Nucl Med 2001;42:213–221.
63. Smith-Jones PM, Stolz B, Bruns C, et al. Gallium-67/gallium-68-[DFO]-octreotide—a potential radiopharmaceutical for PET imaging of somatostatin receptor-positive tumors: synthesis and radiolabeling in vitro and preliminary in vivo studies. J Nucl Med 1994;35:317–325.
64. Guhlke S, Wester H-J, Bruns C, et al. (2-[^{18}F]Fluoropropionyl-D(phe^1)-octreotide, a potential radiopharmaceutical for quantitative somatostatin receptor imaging with PET: synthesis, radiolabeling, in vitro validation and biodistribution in mice. Nucl Med Biol 1994;21:819–825.
65. Brockmann J, Rosch F, Herzog H, et al. In vivo uptake kinetics and dosimetry calculations of 86Y-DTPA-octreotide with PET as a model for potential endotherapeutic octreotides labelled with 90Y. J Labelled Compd Radiopharm 1995;37:519–521.
66. Wester H-J, Brockmann J, Rosch F, et al. PET-pharmacokinetics of ^{18}F-octreotide: a comparison with ^{67}Ga-DFO- and ^{86}Y-DTPA-octreotide. Nucl Med Biol 1997;24:275–286.
67. Stolz B, Smith-Jones PM, Albert R, et al. Biological characterization of [67Ga] or [68Ga] labelled DFO-octreotide (SDZ-216-927) for PET studies of somatostatin receptor positive tumors. Horm Metab Res 1994;26:452–459.
68. Henze M, Schuhmacher J, Hipp P, et al. PET imaging of somatostatin receptors using [^{68}Ga]DOTA-D-Phe^1-Tyr^3-octreotide: first results in patients with meningiomas. J Nucl Med 2001;42:1053–1056.
69. Carraway R, Leeman S. The isolation of a new hypotensive peptide, neurotensin, from bovine hypothalami. J Biol Chem 1973;248:6854–6861.
70. Kitabgi P, Carraway R, Leeman S. Isolation of a tridecapeptide from bovine intestinal tissue and its partial characterization as neurotensin. J Biol Chem 1976;251:7053–7058.
71. Tyler-McMahon B, Boules M, Richelson E. Neurotensin: peptide for next millenium. Regul Pept 2000;93:125–136.
72. Ehlers R, Kim S, Zhang Y, et al. Gut peptide receptor expression in human pancreatic cancers. Ann Surg 2000;231:838–848.
73. Reubi J, Waser B, Friess H, et al. Neurotensin receptors: a new marker for human ductal pancreatic adenocarcinoma. Gut 1998;42:546–550.
74. Chalon P, Vita N, Kaghad M, et al. Molecular cloning of levocabastine-sensitive neurotensin binding site. FEBS Lett 1996;386:91–94.
75. Mazella J, Botto J, Guillemare E, et al. Structure, functional expression, and cerebral localization of the levocabastine-sensitive neurotensin/neuromedin N receptor from mouse brain. J Neurosci 1996;16:5613–5620.
76. Vita N, Oury-Donat F, Chalon P, et al. Neurotensin is an antagonist of the human neurotensin NT_2 receptor expressed in Chinese hampster ovary cells. Eur J Pharmacol 1998;360:265–272.
77. Mazella J, Zsurger N, Navarro V, et al. The 100-KDa neurotensin receptor is gp95/sortilin, a non-G-protein-coupled receptor. J Biol Chem 1998;273:26273–26276.

78. Kitabgi P, Checkler F, Mazella J, et al. Pharmacology and biochemistry of neurotensin receptors. Rev Clin Basic Pharmacol 1985;5:397–486.
79. Chavatte K, Mertens J, Van Den Winkel P. Method for effective ^{201}Tl(III) labelling of diethylenetriamine pentaacetic acid (DTPA)-functionalized peptides: radiosynthesis of ^{201}Tl(III)DTPA-neurotensin(8-13). J Labelled Compd Radiopharm 2000;43:1227–1234.
80. Chavatte K, Wong E, Fauconnier T, et al. Rhenium (Re) and technetium (Tc)-99m oxocomplexes of neurotensin(8-13). J Labelled Compd Radiopharm1999;42:415–421.
81. Blauenstein P, Willmann M, Carrel-Remy N, et al. Pharmacological investigation of metabolically stablized peptides labeled with Technetium-99m [abstract]. Eur J Nucl Med 1999;26:1197.
82. Garcia-Garayoa E, Allemann-Tannahill L, Blauenstein P, et al. *In vitro* and *in vivo* evaluation of new radiolabeled neurotensin(8-13) analogues with high affinity for NT1 receptors. Nucl Med Biol 2001;28:75–84.
83. Bergmann R, Scheunemann M, Heichert C, et al. Biodistribution and catabolism of ^{18}F-labeled neurotensin(8-13) analogs. Nucl Med Biol 2002;29:61–72.
84. Eliceiri B, Cheresh D. Adhesion events in angiogenesis. Curr Opin Cell Biol 2001;13:563–568.
85. Haubner R, Wester H, Burkhart F, et al. Glycosylated RGD-containing peptides: tracer for tumor targeting and angiogenesis imaging with improved biokinetics. J Nucl Med 2001;42:326–336.
86. Breeman W, Hofland L, de Jong M, et al. Evaluation of radiolabelled Bombesin analogues for receptor-targeted scintigraphy and radiotherapy. Int J Cancer 1999;81:658–665.
87. Said S, Mutt V. Polypeptide with broad biological activity: isolation from the small intestine. Science 1970;69:1217–1218.
88. Rao P, Thakur M, Pallela V, et al. ^{99m}Tc labeled VIP analog: evaluation for imaging colorectal cancer. Nucl Med Biol 2001;28:445–450.
89. Virgolini I, Raderer M, Kurtaran A, et al. ^{123}I-vasoactive intestinal peptide (VIP) receptor scanning: update of imaging results in patients with adenocarcinomas and endocrine tumors of the gastrointestinal tract. Nucl Med Biol 1996;23:685–692.
90. Fadok V, Bratton D, Rose D, et al. A receptor for phosphatidylserine-specific clearance of apoptotic cells. Nature 2000;405:85–90.
91. Tait J, Brown D, Gibson D, et al. Development and characterization of annexin V mutants with endogenous chelation for (99m)Tc. Bioconjug Chem 2000;11:918–925.
92. Blankenberg FG, Katsikis PD, Tait JF, et al. *In vivo* detection and imaging of phosphatidylserine expression during programmed cell death. Proc Natl Acad Sci U S A 1998;95:6349–6354.
93. Blankenberg F, Robbins R, Stoot J, et al. Radiolabeled annexin V imaging: diagnosis of allograft rejection in an experimental rodent model of liver transplantation. Radiology 2000;214:795–800.
94. Narula J, Acio E, Narula N, et al. Annexin-V imaging for noninvasive detection of cardiac allograft rejection. Nat Med 2001;7:1347–1352.
95. Pardridge W. Drug and gene targeting to the brain with molecular Trojan horses. Nat Rev Drug Discovery 2002;1:131–139.
96. Kurihara A, Deguchi Y, Pardridge W. Epidermal growth factor radiopharmaceuticals: ^{111}In chelation, conjugation to a blood-brain barrier delivery vector via a biotin-polyethylene linker, pharmacokinetics, and in vivo imaging of experimental brain tumors. Bioconjug Chem 1999;10:502–511.
97. Carrasco N. Iodide transport in the thyroid gland. Biochim Biophys Acta 1993;1154:65–82.
98. Tazebay U, Wapnir I, Levy O, et al. The mammary gland iodide trasnporter is expressed during lactation and in breast cancer. Nat Med 2000;6:871–878.
99. Boland A, Ricard M, Opolon P, et al. Adenovirus-mediated transfer of the thyroid sodium/iodide symporter gene into tumors for a targeted radiotherapy. Cancer Res 2000;60:3484–3492.
100. Spitzweg C, Dietz A, O'Connor M, et al. In vivo sodium iodide symporter gene therapy of prostate cancer. Gene Ther 2001;8:1524–1531.
101. Haberkorn U. Gene therapy with sodium/iodide symporter in hepatocarcinoma. Exp Clin Endocrinol Diabetes 2001;109:60–62.
102. Huang M, Batra R, Kogai T, et al. Ectopic expression of the thyroperoxidase gene augments radioiodide uptake and retention mediated by the sodium iodide symporter in non-small cell lung cancer. Cancer Gene Ther 2001;8:612–618.
103. Moon D, Park K, Park K, et al. Correlation between 99mTc-pertechnetate uptakes and expressions of human sodium iodide symporter gene in breast tumor tissues. Nucl Med Biol 2001;28:829–834.
104. Juliano RL, Ling V. A surface glycoprotein modulating drug permeability in Chinese hamster ovary cell mutants. Biochim Biophys Acta 1976;455:152–162.
105. Gros P, Ben Neriah Y, Croop JM, et al. Isolation and expression of a complementary DNA that confers multidrug resistance. Nature 1996;323:728–731.
106. Shen DW, Fojo A, Chin JE, et al. Human multidrug-resistant cell lines: increased mdr1 expression can precede gene amplification. Science 1986;232:643–645.
107. Gottesman MM, Pastan I. Biochemistry of multidrug resistance mediated by the multidrug transporter. Annu Rev Biochem 1993;62:385–427.
108. Bosch I, Croop J. P-glycoprotein multidrug resistance and cancer. Biochim Biophys Acta 1996;1288:F37–F54.
109. Cole SPC, Bhardwaj G, Gerlach JH, et al. Overexpression of a transporter gene in a multidrug-resistant human lung cancer cell line. Science 1992;258:1650–1654.
110. Flens MJ, Zaman GJR, van der Valk P, et al. Tissue distribution of multidrug resistance protein. Am J Pathol 1996;148:1237–1247.
111. Gottesman M, Fojo T, Bates S. Multidrug resistance in cancer: role of ATP-dependent transporters. Nat Rev Cancer 2002;2:48–58.
112. Keppler D, Leier I, Jedlitschky G. Transport of glutathione conjugates and glucuronides by the multidrug resistance proteins MRP1 and MRP2. Biol Chem 1997;378:787–791.
113. Lautier D, Canitrot Y, Deeley R, et al. Multidrug resistance mediated by the multidrug resistance protein (*MRP*) gene. Biochem Pharmacol 1996;52:967–977.
114. Scheper R, Broxterman H, Scheffer G, et al. Overexpression of a M_r 110,000 vesicular protein in non-P-glycoprotein-mediated multidrug resistance. Cancer Res 1993;53:1475–1479.
115. Doyle L, Yang W, Abruzzo L, et al. A multidrug resistance transporter from human MCF-7 breast cancer cells. Proc Natl Acad Sci U S A 1998;95:15665–15670.
116. Miyake K, Mickley L, Litman T, et al. Molecular cloning of cDNAs which are highly overexpressed in mitoxantrone-resistant cells: demonstration of homology to ABC transport genes. Cancer Res 1999;59:8–13.
117. Allikmets R, Schrimi L, Hutchinson A, et al. A human placenta-specific ATP-binding cassette gene (*ABCP*) on chromosome 4q22 that is involved in multidrug resistance. Cancer Res 1998;58:5337–5339.
118. Ford JM, Hait WN. Pharmacology of drugs that alter multidrug resistance in cancer. Pharmacol Rev 1990;42:155–199.
119. Gaveriaux C, Boesch D, Jachez B. PSC 833, a non-immunosuppressive cyclosporin analog, is a very potent multidrug-resistance modifier. J Cell Pharmacol 1991;2:225–234.
120. Hyafil F, Vergely C, Du Vignaud P, et al. *In vitro* and *in vivo* reversal of multidrug resistance by GF120918, an acridonecarboxamide derivative. Cancer Res 1993;53:4595–4602.
121. Dantzig A, Shepard R, Cao J, et al. Reversal of P-glycoprotein-mediated multidrug resistance by a potent cyclopropyldibenzosuberane modulator, LY335979. Cancer Res 1996;56:4171–4179.
122. Germann U, Ford P, Schlakhter D, et al. Chemosensitization and drug accumulation effects of VX-710, verapamil, cyclosporin A, MS-209, and GF120918 in multidrug resistant HL60/ADR cells expressing the multidrug resistance-associated protein MRP. Anticancer Drugs 1997;8:141–155.
123. Rabindran S, He H, Singh M, et al. Reversal of a novel multidrug resistance mechanism in human colon carcinoma cells by fumitremorgin C. Cancer Res 1998;58:5850–5858.
124. Newman M, Rodarte J, Benbatoul K, et al. Discovery and characterization of OC144-093, a novel inhibitor of P-glycoprotein-mediated multidrug resistance. Cancer Res 2000;60:2964–2972.
125. Sorrentino B, Brandt S, Bodine D, et al. Selection of drug-resistant bone marrow cells in vivo after retroviral transfer of human MDR1. Science 1992;257:99–103.
126. Podda S, Ward M, Himelstein A, et al. Transfer and expression of the human multiple drug resistance gene into live mice. Proc Natl Acad Sci U S A 1992;89:9676–9680.
127. Hanania E, Fu S, Roninson I, et al. Resistance to taxol chemotherapy produced in mouse marrow cells by safety-modified retroviruses containing a human MDR-1 transcription unit. Gene Ther 1995;2:279–284.

128. Moscow J, Huang H, Carter C, et al. Engraftment of MDR1 and NeoR gene-transduced hematopoietic cells after breast cancer chemotherapy. Blood 1999;94:52–61.
129. Piwnica-Worms D. Functional identification of multidrug resistance gene expression in vivo. In: American Society of Clinical Oncology, Educational Book. Baltimore: Lippincott Williams & Wilkins; Spring 2000. p 178–184.
130. Piwnica-Worms D, Chiu M, Budding M, et al. Functional imaging of multidrug-resistant P-glycoprotein with an organotechnetium complex. Cancer Res 1993;53:977–984.
131. Piwnica-Worms D, Rao V, Kronauge J, et al. Characterization of multidrug-resistance P-glycoprotein transport function with an organotechnetium cation. Biochemistry 1995;34:12210–12220.
132. Ballinger J, Hua H, Berry B, et al. ^{99m}Tc-sestamibi as an agent for imaging P-glycoprotein-mediated multi-drug resistance: *in vitro* and *in vivo* studies in a rat breast tumour cell line and its doxorubicin-resistant variant. Nucl Med Comm 1995;16:253–257.
133. Ballinger JR, Sheldon KM, Boxen I, et al. Differences between accumulation of Tc-99m-MIBI and Tl-201-thallous chloride in tumor cells: role of P-glycoprotein. Q J Nucl Med 1995;39:122–128.
134. Cordobes M, Starzec A, Delmon-Moingeon L, et al. Technetium-99m-sestamibi uptake by human benign and malignant breast tumor cells: correlation with *mdr* gene expression. J Nucl Med 1996;37:286–289.
135. Herman LW, Sharma V, Kronauge JF, et al. Novel hexakis(areneisonitrile)technetium(I) complexes as radioligands targeted to the multidrug resistance P-glycoprotein. J Med Chem 1995;38:2955–2963.
136. Ballinger JR, Bannerman J, Boxen I, et al. Technetium-99m-tetrofosmin as a substrate for P-glycoprotein: in vitro studies in multidrug-resistant breast tumor cells. J Nucl Med 1996;37:1578–1582.
137. Luker G, Rao V, Crankshaw C, et al. Characterization of phosphine complexes of technetium (III) as transport substrates of the multidrug resistance (MDR1) P-glycoprotein and functional markers of P-glycoprotein at the blood-brain barrier. Biochemistry 1997;36:14218–14227.
138. Ballinger J, Muzzammil T, Moore M. Technetium-99m-furifosmin as an agent for functional imaging of multidrug resistance in tumors. J Nucl Med 1997;38:1915–1919.
139. Crankshaw C, Marmion M, Luker G, et al. Novel Tc(III)-Q-complexes for functional imaging of the multidrug resistance (*MDR1*) P-glycoprotein. J Nucl Med 1998;39:77–86.
140. Chen W, Luker K, Dahlheimer J, et al. Effects of *MDR1* and *MDR3* P-glycoproteins, MRP1 and BCRP/MXR/ABCP on transport of Tc-99m-tetrofosmin. Biochem Pharmacol 2000;60:413–426.
141. Dyszlewski M, Blake H, Dalheimer J, et al. Characterization of a novel Tc-99m-carbonyl complex as a functional probe of *MDR1* P-glycoprotein transport activity. Mol Imaging 2001;1:24–35.
142. Piwnica-Worms D, Kronauge J, Chiu M. Uptake and retention of hexakis (2-methoxy isobutyl isonitrile) technetium(I) in cultured chick myocardial cells: mitochondrial and plasma membrane potential dependence. Circulation 1990;82:1826–1838.
143. Sharma V, Beatty A, Wey S-P, et al. Novel gallium(III) complexes transported by *MDR1* P-glycoprotein: potential PET imaging agents for probing P-glycoprotein-mediated transport activity in vivo. Chem Biol 2000;7:335–343.
144. Hendrikse N, Franssen E, van der Graaf W, et al. Visualization of multidrug resistance in vivo. Eur J Nucl Med 1999;26:283–293.
145. Hendrikse N, de Vries EG, Eriks-Fluks L, et al. A new in vivo method to study P-glycoprotein transport in tumors and the blood-brain barrier. Cancer Res 1999;59:2411–2416.
146. Levchenko A, Mehta B, Lee J-B, et al. Evaluation of ^{11}C-colchicine for PET imaging of multiple drug resistance. J Nucl Med 2000;41:493–501.
147. Kiesewetter D, Eckelman W. Radiochemical synthesis of [18F]fluoropaclitaxel [abstract]. J Labelled Compd Radiopharm 2001;44:S903–S905.
148. Packard A, Barbarics E, Kronauge J, et al. Copper(II)diiminedioxime complexes for imaging multidrug resistance. In: Proceedings of the 215th American Chemical Society Meeting 1998, Washington, DC, Nucl-100.
149. Zweit J, Lewis J, Dearling J, et al. Copper-64-diphosphine complexes: potential PET tracers for the assessment of multidrug resistance in tumors [abstract]. J Nucl Med 1997;38:133P.
150. Blower P. Small coordination compounds as radiopharmaceuticals for cancer targeting. Transition Met Chem 1998;23:109–112.
151. Lewis J, Dearling J, Sosabowski J, et al. Copper bis(diphosphine)complexes: radiopharmaceuticals for detection of multidrug resistance in tumors by PET. Eur J Nucl Med 2000;27:638–646.
152. Bigott H, McCarthy D, Wust F, et al. Production, processing and uses of 94m-Tc. J Labelled Compd Radiopharm 2001;44:S119–S121.
153. Del Vecchio S, Ciarmiello A, Potena MI, et al. In vivo detection of multidrug resistance (MDR1) phenotype by technetium-99m-sestamibi scan in untreated breast cancer patients. Eur J Nucl Med 1997;24:150–159.
154. Del Vecchio S, Ciarmiello A, Pace L, et al. Fractional retention of technetium-99m-sestamibi as an index of P-glycoprotein expression in untreated breast cancer patients. J Nucl Med 1997;38:1348–1351.
155. Chen C, Meadows B, Regis J, et al. Detection of in vivo P-glycoprotein inhibition by PSC 833 using Tc-99m-sestamibi. Clin Cancer Res 1997;3:545–552.
156. Luker GD, Fracasso PM, Dobkin J, et al. Modulation of the multidrug resistance P-glycoprotein: detection with Tc-99m-sestamibi in vivo. J Nucl Med 1997;38:369–372.
157. Bom H, Kim Y, Lim S, et al. Dipyridamole modulated Tc-99m-sestamibi (mibi) scintigraphy: a predictor of response to chemotherapy in patients with small cell lung cancer [abstract]. J Nucl Med 1997;38:240P.
158. Kostakoglu L, Elahi N, Kirarli P, et al. Clinical validation of the influence of P-glycoprotein on technetium-99m-sestamibi uptake in malignant tumors. J Nucl Med 1994;38:1003–1008.
159. Barbarics E, Kronauge J, Cohen D, et al. Characterization of P-glycoprotein transport and inhibition in vivo. Cancer Res 1998;58:276–282.
160. Kostakoglu L, Kirath P, Ruacan S, et al. Association of tumor washout rates and accumulation of technetium-99m-MIBI with expression of P-glycoprotein in lung cancer. J Nucl Med 1998;39:228–234.
161. Ciarmiello A, Del Vecchio S, Silvestro P, et al. Tumor clearance of technetium-99m-sestamibi as a predictor of response to neoadjuvant chemotherapy for locally advanced breast cancer. J Clin Oncol 1998;16:1677–1683.
162. Fukumoto M, Yoshida D, Hayase N, et al. Scintigraphic prediction of resistance to radiation and chemotherapy in patients with lung carcinoma: technetium 99m-tetrofosmin and thallium-201 dual single photon emission computed tomography study. Cancer 1999;86:1470–1479.
163. Nagamachi S, Jinnouchi S, Ohnishi T, et al. The usefulness of Tc-99m-MIBI for evaluating brain tumors: comparative study with Tl-201 and relation with P-glycoprotein. Clin Nucl Med 1999;24:765–772.
164. Zhou J, Higashi K, Ueda Y, et al. Expression of multidrug resistance protein and messenger RNA correlate with ^{99m}Tc-MIBI imaging in patients with lung cancer. J Nucl Med 2001;42:1476–1483.
165. Hendrikse N, Franssen E, van der Graaf W, et al. ^{99m}Tc-sestamibi is a substrate for P-glycoprotein and the multidrug resistance-associated protein. Br J Cancer 1998;77:353–358.
166. Peck R, Hewett J, Harding M, et al. Phase I and pharmacokinetic study of the novel MDR1 and MRP1 inhibitor biricodar administered alone and in combination with doxorubicin. J Clin Oncol 2001;19:3130–3141.
167. Wu A, Yazaki P, Tsai S, et al. High-resolution microPET imaging of carcinoembryonic antigen-positive xenografts by using a copper-64-labeled engineered antibody fragment. Proc Natl Acad Sci U S A 2000;97:8495–8500.
168. Derossi D, Calvet S, Trembleau A, et al. Cell internalization of the third helix of the Antennapedia homeodomain is receptor-independent. J Biol Chem 1996;271:18188–18193.
169. Elliot G, O'Hare P. Intercellular trafficking and protein delivery by a herpesvirus structural protein. Cell 1997;88:223–233.
170. Kubota S, Siomi H, Satoh T, et al. Functional similarity of HIV-1 rev and HTLV-1 rex proteins: identification of a new nucleolar-targeting signal in rev protein. Biochem Biophys Res Comm 1989;162:963–970.
171. Frankel A, Pabo C. Cellular uptake of the tat protein from human immunodeficiency virus. Cell 1988;55:1189–1193.
172. Fawell S, Seery J, Daikh Y, et al. Tat-mediated delivery of heterologous proteins into cells. Proc Natl Acad Sci U S A 1994;91:664–668.

173. Nagahara H, Vocero-Akbani A, Synder E, et al. Transduction of full-length TAT fusion proteins directly into mammalian cells: TAT-p27^{Kip1} induces cell migration. Nat Med 1998;4:1449–1452.
174. Vives E, Brodin P, Lebleu B. A truncated HIV-1 Tat protein basic domain rapidly translocates through the plasma membrane and accumulates in the cell nucleus. J Biol Chem 1997;272:16010–16017.
175. Josephson L, Tung C-H, Moore A, et al. High-efficiency intracellular magnetic labeling with novel superparamagnetic-Tat peptide conjugates. Bioconjug Chem 1999;10:186–191.
176. Polyakov V, Sharma V, Dahlheimer J, et al. Synthesis and characterization in vitro of membrane permeant peptide conjugates for imaging and radiotherapy. J Labelled Compd Radiopharm 1999; 42:S4–S6.
177. Polyakov V, Sharma V, Dahlheimer J, et al. Novel Tat-peptide chelates for direct transduction of technetium-99m and rhenium into human cells for imaging and radiotherapy. Bioconjug Chem 2000;11:762–771.
178. Vocero-Akbani A, Heyden N, Lissy N, et al. Killing HIV-infected cells by transduction with an HIV protease-activated caspase-3 protein. Nat Med 1999;5:29–33.
179. Schwarze S, Ho A, Vocero-Akbani A, et al. In vivo protein transduction: delivery of a biologically active protein into the mouse. Science 1999;285:1569–1572.
180. Herschman H, Barrio J, Satyamurthy N, et al. Progress toward in vivo imaging of reporter gene expression using positron emission tomography. In: American Society of Clinical Oncology, Educational Book, Spring 2000. Baltimore: Lippincott Williams & Wilkins, p 169–177.
181. Liang Q, Satyamurthy N, Barrio J, et al. Noninvasive, quantitative imaging in living animals of a mutant dopamine D2 receptor reporter gene in which ligand binding is uncoupled from signal transduction. Gene Ther 2001;19:1490–1498.
182. Zinn K, Buchsbaum D, Chaudhuri T, et al. Noninvasive monitoring of gene transfer using a reporter receptor imaged with a high-affinity peptide radiolabeled with Tc-99m or Re-188. J Nucl Med 2000;41:887–895.
183. Hemminki A, Zinn K, Liu B, et al. In vivo molecular chemotherapy and noninvasive imaging with an infectivity-enhanced adenovirus. J Natl Cancer Inst 2002;94:741–749.
184. Zhang L, Adams J, Billick E, et al. Molecular engineering of a two-step transcription amplification (TSTA) system for transgene delivery in prostate cancer. Mol Ther 2002;5:223–232.
185. Maclaren D, Gambhir S, Satyamurthy N, et al. Repetitive, noninvasive imaging of the dopamine D2 receptor as a reporter gene in living animals. Gene Ther 1999;6:785–791.
186. Yu Y, Annala A, Barrio J, et al. Quantification of target gene expression by imaging reporter gene expression in living animals. Nat Med 2000;6:933–937.
187. Chaudhuri T, Rogers B, Buchsbaum D, et al. A noninvasive reporter system to image adenoviral-mediated gene transfer to ovarian cancer xenografts. Gynecol Oncol 2001;83:432–438.
188. Haberkorn U, Oberdorfer F, Gebert J, et al. Monitoring gene therapy with cytosine deaminase: in vitro studies using tritiated-5-fluorocytosine. J Nucl Med 1996;37:87–94.
189. Haubner R, Avril N, Hantzopoulos P, et al. In vivo imaging of herpes simplex virus type 1 thymidine kinase gene expression: early kinetics of radiolabelled FIAU. Eur J Nucl Med 2000;27:283–291.
190. Tomicic M, Thust R, Sobol R, et al. DNA polymerase β mediates protection of mammalian cells against ganciclovir-induced cytotoxicity and DNA breakage. Cancer Res 2001;61:7399–7403.
191. Saito Y, Price R, Rottenberg D, et al. Quantitative autoradiographic mapping of herpes simplex virus encephalitis with a radiolabeled antiviral drug. Science 1982;217:1151–1153.
192. Saito Y, Rubenstein R, Price R, et al. Diagnostic imaging of herpes simplex virus encephalitis using a radiolabeled antiviral drug: autoradiographic assessment in an animal model. Ann Neurol 1984;15:548–558.
193. Alauddin M, Conti P. Synthesis and preliminary evaluation of 9-(4-[^{18}F]-fluoro-3-hydroxymethylbutyl)guanine ([^{18}F]FHBG): a new potential imaging agent for viral infection and gene therapy using PET. Nucl Med Biol 1998;25:175–180.
194. Blasberg R, Tjuvajev J. Herpes simplex virus thymidine kinase as a marker/reporter gene for PET imaging of gene therapy. Q J Nucl Med 1999;43:163–169.
195. Gambhir S, Barrio J, Herschman H, et al. Assays for noninvasive imaging of reporter gene expression. Nucl Med Biol 1999;26:481–490.
196. Charziioannou A, Cherry S, Shao Y, et al. Performance evaluation of microPET: a high-resolution lutetium oxyorthosilicate PET scanner for animal imaging. J Nucl Med 1999;40:1164–1175.
197. Gambhir S, Barrio J, Phelps M, et al. Imaging adenoviral-directed reporter gene expression in living animals with positron emission tomography. Proc Natl Acad Sci U S A 1999;96:2333–2338.
198. Shao Y, Cherry S, Farahani K, et al. Simultaneous PET and MR imaging. Phys Med Biol 1997;42:1965–1970.
199. Hospers G, Calogero A, van Waarde A, et al. Monitoring of herpes simplex virus thymidine kinase enzyme activity using positron emission tomography. Cancer Res 2000;60:1488–1491.
200. Gambhir S, Bauer E, Black M, et al. A mutant herpes simplex virus type 1 thymidine kinase reporter gene shows improved sensitivity for imaging reporter gene expression with positron emission tomography. Proc Natl Acad Sci U S A 2000;97:2785–2790.
201. Tjuvajev J, Chen S, Joshi A, et al. Imaging adenoviral-mediated herpes virus thymidine kinase gene transfer and expression in vivo. Cancer Res 1999;59:5186–5193.
202. Luker G, Luker K, Sharma V, et al. *In vitro* and *in vivo* characterization of a dual-function green fluorescent protein-HSV1-thymidine kinase reporter gene driven by the human elongation factor 1α promoter. Mol Imaging 2001;1:65–73.
203. Ponomarev V, Doubrovin M, Lyddane C, et al. Imaging TCR-dependent NFAT-mediated T-cell activation with positron emission tomography in vivo. Neoplasia 2001;3:480–488.
204. Doubrovin M, Ponomarev V, Beresten T, et al. Imaging transcriptional regulation of p53-dependent genes with positron emission tomography *in vivo*. Proc Natl Acad Sci U S A 2001;98:9300–9305.
205. Luker G, Sharma V, Pica C, et al. Non-invasive imaging of protein-protein interactions in living animals. Proc Natl Acad Sci U S A 2002;99:6961–6966.
206. Braun K, Degen J, Sandgren E. Hepatocyte transplantation in a model of toxin-induced liver disease: variable therapeutic effect during replacement of damaged parenchema by donor cells. Nat Med 2000;6:320–326.
207. Green L, Yap C, Nguyen K, et al. Indirect monitoring of endogenous gene expression by positron emission tomography (PET) imaging of reporter gene expression in transgenic mice. Mol Imaging Biol 2002;4:71–81.